NASA TECHNICAL MEMORANDUM

NASA TM X-62,176

NASA TM X-62,176

AN ANALYSIS OF THE TAKEOFF AND LANDING PERFORMANCE OF A JET–POWERED STOL AUGMENTOR WING DESIGN

Susan E. Post, Bruno J. Gambucci, and Curt A. Holzhauser

Ames Research Center
and
U.S. Army Air Mobility R&D Laboratory
Moffett Field, Calif. 94035

August 1972

64

INTRODUCTION

This report presents a preliminary study of the takeoff and landing performance characteristics of a swept wing airplane with augmented jet flap, designed for STOL operation and low noise. The study is based on aerodynamic data from wind tunnel tests of a large-scale swept augmentor wing model, scaled up to a 48,000 pound airplane. This wind tunnel data is documented in reference 1. Engine characteristics are based on a turbo fan with a fan pressure ratio of 2.5 delivering the major portion of the thrust to the augmentor flap. A description of the overall airplane configuration, the propulsion system, and the use of the aerodynamics is presented.

To assess the STOL performance of the airplane, takeoff and landing distances and flight path capabilities were computed at various flap deflections and thrust levels. After evaluating these results in terms of desired STOL performance with required margins, basic takeoff and landing configurations were chosen. In the sections that follow, these basic configurations are presented with their performance results. For takeoff a summary is given of optimization of the rotation maneuver. Included also is a summary of the effect of gross weight, flap deflection, and thrust level on takeoff performance.

NOTATION

a_n	Normal acceleration, ft/sec^2
b	Wing span, ft
$\bar{c}$	Mean aerodynamic chord, ft
C_D	Drag coefficient, exclusive of ram drag of engines
C_{J_I}	Isentropic jet thrust coefficient, T_C/qS
C_L	Lift coefficient, exclusive of net hot thrust
C_m	Pitching moment coefficient
C_{Lmax}	Maximum lift coefficient
C_l	Rolling moment coefficient
C_n	Yawing moment coefficient
h	Altitude, ft
$\dot{h}$	Vertical velocity, ft/sec
i_T	Horizontal tail incidence, positive with leading edge up, deg
L	Rolling moment, ft-lb
l_{eng}	Lateral distance to engine
N	Yawing moment, ft-lb
q	Dynamic pressure, lb/ft^2
R/C	Rate of climb, ft/sec
R/S	Rate of sink, ft/sec
S	Wing area, ft^2
s	Distance, ft
T_C	Cold thrust, lb
T_H	Hot thrust, lb

V	Velocity in body axes, knots
V_j	Jet exhaust velocity, fps
V_{LOF}	Lift off velocity, knots
V_{MC}	Minimum control velocity, knots
Vmin	Minimum velocity, knots
V_R, V_{ROT}	Rotation velocity, knots
V_{Rmin}	Minimum rotation velocity, knots
V_S	Stall speed, knots
V_1	Decision velocity on takeoff, knots
V_2	Climbout velocity, knots
V_{35}	Velocity at 35 foot threshold, knots
δ_a	Aileron deflection, positive with trailing edge down, deg
δ_e	Elevator deflection, positive with trailing edge down, deg
δ_f	Augmentor flap deflection, positive with trailing edge down, deg
δ_s	Slat deflection, positive with leading edge down, deg
γ	Flight path angle, deg
μ_B	Braking coefficient
μ_R	Rolling friction coefficient
ν	Thrust deflection angle, positive down, deg
α	Angle of attack, deg
α_M	Maximum commanded angle of attack, deg

DESCRIPTION OF AIRCRAFT CONFIGURATION

Geometry

A sketch of the aircraft studied is given in figure 1. It is a jet powered STOL configuration with the fan air ducted through the wing and ejected through an augmentor flap. The design is similar to that reported in reference 1, having the wing swept back 27.5° and an aspect ratio of 8. It has been assumed that the aircraft weighs 48,000 pounds, which corresponds to a wing loading of 80 pounds per square foot. The propulsion system, described later, provides an uninstalled thrust-to-weight ratio of 0.38.

High-Lift and Control System

A cross section of the augmentor flap tested in reference 1 is shown in figure 2. The flaps extend from 12 to 70 percent of the semispan, and they deflect 70°. The ailerons are drooped symmetrically 30°. A full span leading-edge slat, deflected 60°, is employed.

Blowing BLC is provided to the ailerons to maintain attached flow when they are deflected for lateral control. Five percent of the fan air is allocated for BLC. Additional lateral control is provided by spoilers located forward of the flaps and by surfaces within the augmentors that choke the flow. The spoilers and chokes are also deployed symmetrically when the aircraft is on the ground to spoil wing lift for more effective braking.

Directional control is achieved by a double hinged rudder that deflects to 50°.

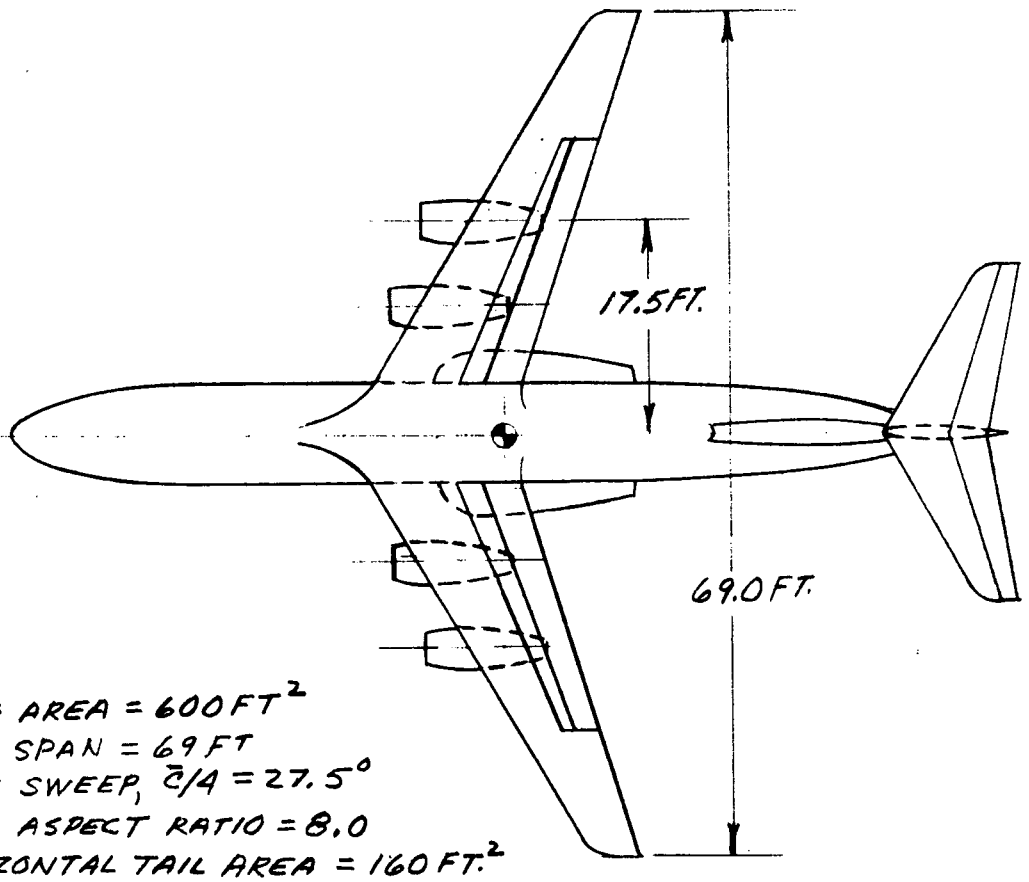

WING AREA = 600 FT^2
WING SPAN = 69 FT
WING SWEEP, $\bar{c}/4 = 27.5^0$
WING ASPECT RATIO = 8.0
HORIZONTAL TAIL AREA = 160 FT.^{2}
VERTICAL TAIL AREA = 120 FT^2
NOMINAL GROSS WEIGHT = 48000 LBS
WING LOADING = 80 LB/FT^2
THRUST/WEIGHT = 0.38
$\bar{c}$ = 9.46 FT.

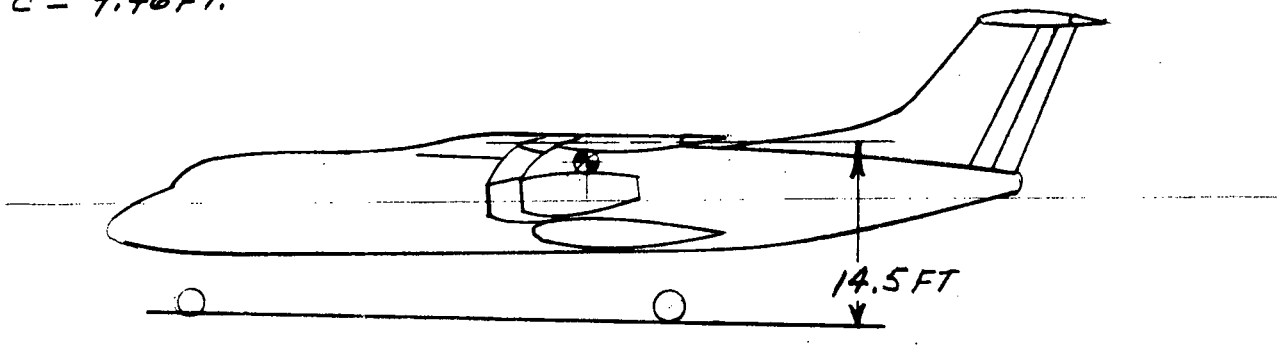

FIGURE 1.- AUGMENTOR WING STOL CONFIGURATION.

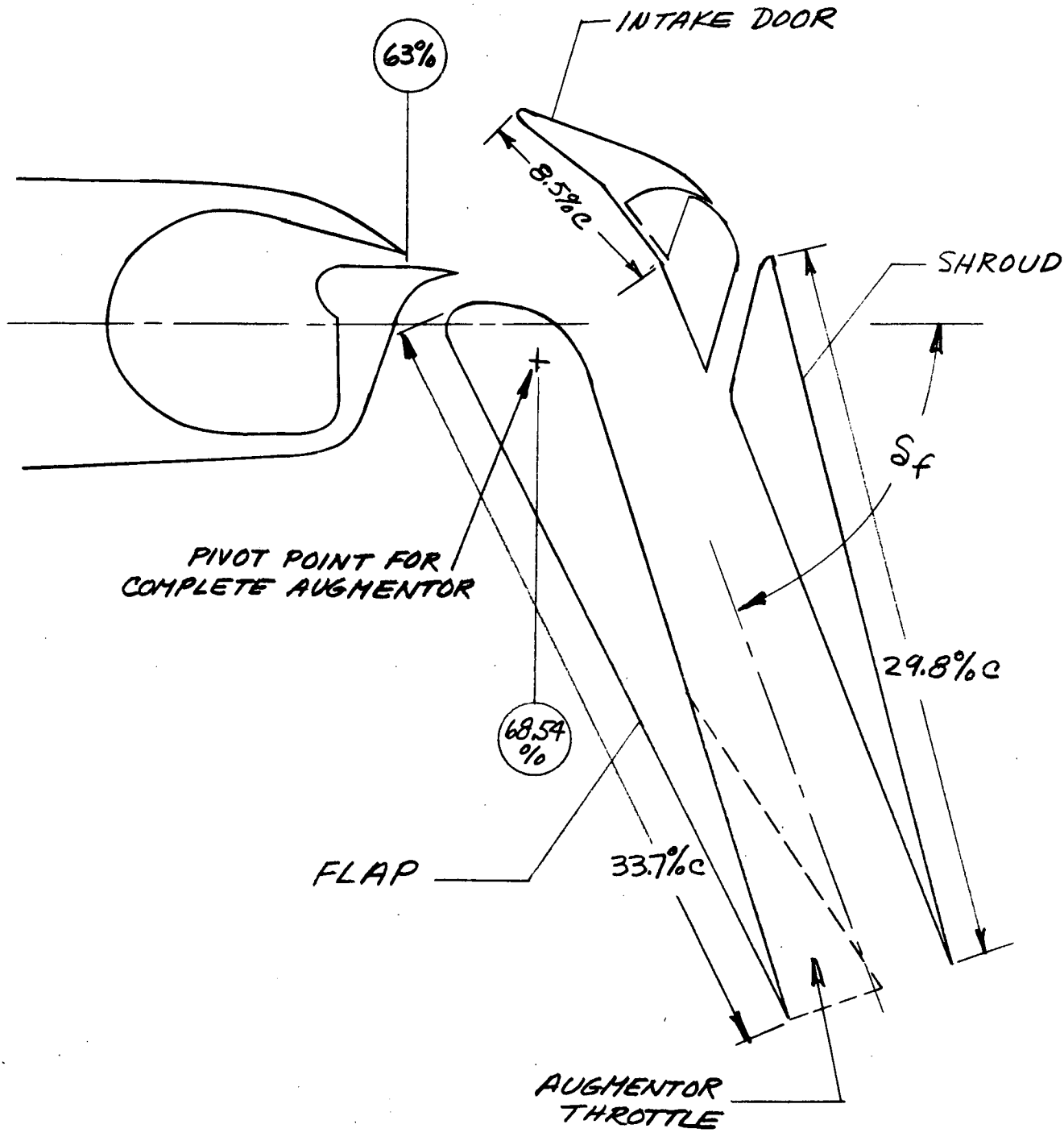

FIGURE 2.- STREAMWISE SECTION OF AUGMENTOR FLAP.

The horizontal tail is deflected as the flaps are deflected to trim a major portion of the pitching moment. The elevator can be deflected 45° for control.

Propulsion System

The engine assumed for the major part of this study is a two-stream engine with an uninstalled thrust level of 4600 pounds for each engine, and with 78% of this thrust in the cold stream. The cold air flow, delivered with a pressure ratio of about 2.5, is ducted through the nacelle and wing and ejected into the augmentor flap system in the manner described in reference 2. An 8% thrust loss (15% total pressure loss) is estimated for the duct loss of the cold air between the engine and the plenum chamber prior to the discharge into the ejector system. Five percent of this air is used for boundary layer control of the aileron. The remaining 22% of the thrust obtained from the hot gas is exited with low velocity to reduce noise. A deflectable nozzle is installed at the hot gas exit to deflect the thrust from 0° (thrusting) to 120° (braking). A 3% installation loss was assumed. The total engine airflow was 140 pounds per second for each engine at maximum thrust. The base case is a total uninstalled thrust-to-weight ratio of 0.38 with a ratio of net installed cold to total thrust of 74%.

The takeoff performance for a three-stream engine was also determined. This engine had an uninstalled thrust-to-weight ratio of 0.38 and is similar to that described in reference 3. Thirty-seven percent of the thrust at a pressure ratio of about 2.5 was used for wing flow, 26% hot thrust and 37% cold thrust at a pressure ratio of about 1.4 exited directly aft. The duct and exit assumptions were the same as used for the two-stream engine.

Noise Characteristics

The thrust split between hot and cold thrust was chosen to provide good aerodynamic characteristics with low noise levels. The pressure ratio of 2.5 was used to permit the cold flow to be accommodated within the wing confines and also to be amenable to the noise attenuation studied in references 2 to 5. Those references presented the results of a design integration and noise study for a 189,000 pound augmentor wing aircraft that was designed for a 2000 foot field length and a noise level of 90 PNdB for a 1978 augmentor wing airplane. The following estimates of components contributing to the 500 foot sideline noise levels were given, along with the tested treatments on which they were based:

W = 189,000 pounds

T = 18,640 pounds/engine

Noise Source	Untreated	Treated	Treatment
Inlet	115 PNdB	90 PNdB	Sonic Choke
Primary Jet	90 PNdB		V_j = 780 feet per second
Augmentor	116 PNdB	90 PNdB	Multilobed nozzle plus tuned lining in the augmentor

On the basis of this information, it can be surmised that the 48,000 pound aircraft of this study would either have a lower noise level for the equivalent treatment or could achieve 90 PNdB with much less treatment of inlet and augmentor flaps.

The Aerodynamics

The aerodynamic data are based on 1971 wind tunnel tests of a large-scale swept augmentor wing model, documented in reference 1. The subset of the data used was for:

δ_f = 31.8°, 41.1°, 51.1°, 70.6°

δ_s = 60°

δ_a = 30°

δ_e = -30° to +10°

i_T = -1° and -10°

The data were available at isentropic jet thrust coefficients (C_{J_I}) from 0. to 1.47.

Some adjustments to the data were made for this study. The pitching moment coefficients were presented for a moment center at .25$\bar{c}$ and .2$\bar{c}$ below the wing chord. These were recomputed for center of gravity at .35$\bar{c}$ and .2$\bar{c}$ below the wing chord. To provide pitching moment coefficients for a tail incidence near trim with an undeflected elevator and an unstalled tail, some adjustment and extrapolation were required. The majority of the data were available at i_T = - 1° and δ_e = -15° with no tail stall evident. It was determined that this condition was equivalent to i_T = -8.7°with undeflected elevator, which provided the desired tail incidence for takeoff and landing. The data with tail on at 31.8° and 51.1° flap deflections were only available at i_T = -10° and δ_e = -15°, conditions where the tail was stalled for a portion of the angle of attack range. Pitching moment coefficients with unstalled tail were estimated for the 31.8° and 51.1° flap deflections.

The adjustments to pitching moment and some extrapolation in C_{J_I} to handle high thrust, low speed situations resulted in the following data set:

δ_f = 31.8°, 41.1°, 51.1°, 70.6°

δ_s = 60°

δ_a = 30°

δ_e = 0°

i_T = -8.7°

C_{J_I} = 0. to 2.4

The wind tunnel data were uncorrected for strut drag, and it is assumed that the data correspond to a gear down situation. The drag coefficients were reduced by an increment of 0.02 to simulate the gear up situation. The final C_L vs α, C_D, C_m curves are shown in Appendix A for flaps 41.1° and 70.6°, gear down.

The pitching moments used for control during takeoff and landing were calculated for an elevator deflection of 45° assuming linear effectiveness and no tail stall. These assumptions were verified by the tests of reference 6 which were done with the same model as used for reference 1, but with a more effective elevator and an inverted slat on the leading edge of the stabilizer. The effects of elevator deflection were taken as:

$\partial C_L/\partial \delta_e$ = .0078/deg

$\partial C_D/\partial \delta_e$ = 0.

$\partial C_m/\partial \delta_e$ = -.0293/deg

The wind tunnel data were based on isentropic jet thrust coefficients, C_{J_I}. Static measurements showed that the isentropic augmentation ratio was about 1.10, and the nozzle efficiency was less than 90% (reference 6).

For the performance calculations of this study it was assumed that the augmentation ratio could be improved 10% and the nozzle efficiency 5% (values demonstrated in reference 4), and that these improvements would be reflected in the aerodynamics over the speed range of interest. The effect of these improvements was assumed to be equivalent to basing the aerodynamics on a reduced C_{J_I} computed as:

$$C_{J_I}\text{new} = C_{J_I}\text{wind tunnel} \times \frac{1.10}{1.25}$$

The resulting C_J's were:

C_{J_I}new	C_{J_I}wind tunnel
0.	0.
.317	.36
.678	.77
.968	1.10
1.294	1.47
1.76	2.0
2.11	2.4

The new C_J's were used to look up aerodynamics throughout the performance calculations. With the improved augmentor system, the same lift is developed with less cold thrust. Note that the aerodynamic data in the appendix is shown in terms of the original wind tunnel C_{J_I}'s.

The test data available was without ground effect and for a model without wing mounted engines. No adjustments were made to include these effects. Recent data (reference 10) were taken with the same model tested near the tunnel floor and with engines installed to simulate the propulsion system and a deflection system. These data, summarized in Appendix C, showed that there were improvements in lift and accelerating force during the takeoff

roll and climb over the 35 foot obstacle. The data corresponding to a landing configuration at an $h/\bar{c} = 2$ (landing gear 5 feet from the ground) showed no lift and drag changes compared to data taken at the tunnel centerline. Installation of wing mounted engines caused a small decrement in lift.

Minimum Control Speed

Minimum control speed for the airplane may be shown to be substantially less than the three engine stall in any configuration. This is a result of the small asymmetry caused by an an engine failure. Since the fan air going to the flaps is assumed to be completely interconnected, any asymmetry is a result of the primary (hot) jet thrust only, 26% of the total engine thrust. The effect of losing an engine on roll and yaw moment is:

$$\Delta L = T_H \times \sin\nu \times l_{eng}$$

$$\Delta N = T_H \times \cos\nu \times l_{eng}$$

where ν is the thrust deflection angle. For takeoff ν is zero so ΔL is zero; ΔN is 18,550 ft-lb, the yaw increment for an outboard engine lost at full power (1060 lb x 17.5 ft). For landing, $\nu = 90$ and the converse is true: ΔL is 18,550 ft-lb.

The compensating roll and yaw increment available with lateral and directional controls at various coefficients and velocities is shown below.

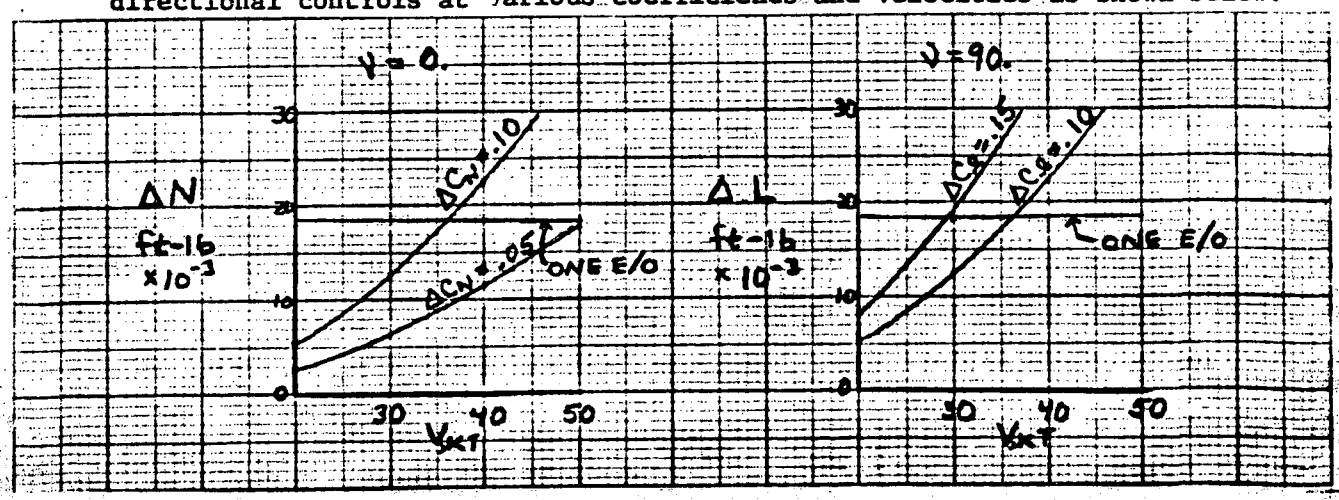

The lowest three-engine stall speed that can be reached with this airplane is about 50 knots. That requires full thrust at 70.6° flap and hot thrust deflected 90°. As may be seen in the sketches above, the minimum control speed may be kept below 50 knots by incremental moment coefficients of just over .05, ignoring control cross coupling and sideslip characteristics. Devices achieving increments of .05 to .10 in yawing moment coefficient and .10 to .15 in rolling moment coefficient have been demonstrated previously on STOL aircraft. Examples are double hinged rudders, ailerons with BLC, and spoilers (references 6 and 7). We will assume employment of such devices on the swept augmentor wing sufficient to maintain V_{MC} less than 50 knots for all configurations and less than 40 knots when $\nu = 90$.

Computation

The takeoff and landing performance calculations presented in this report were done using a static trim program and dynamic takeoff and landing programs run on an IBM 360. All three programs are specifically structured for powered-lift aircraft where aerodynamics are a function of thrust and velocity (C_J) as well as angle of attack and flap deflection. Using these programs, which are described in some detail in Appendix B, takeoff and landing distances and flight path capabilities were computed at various flap deflections and thrust levels. Limited optimization of rotation velocity and maximum rotation angle was carried out in computing the takeoff distances. These various results were evaluated in terms of desired STOL performance and the tentative ground rules for STOL operation

presented in references 7 and 8. Basic takeoff, landing, and pre-approach configurations were then selected for presentation with their respective performance results.

RESULTS

Takeoff

Takeoff Performance

Inspection of the aerodynamic data indicated that two takeoff flap settings were available, 31.8° and 41.1°. The higher flap deflections were not suitable for takeoff with a thrust-to-weight ratio of 0.38 and a 74/26 thrust split. Takeoff performance calculations were done at both flap settings at the baseline thrust (T/W = .38). The flap 41.1° was found to require less field length and was taken as the standard takeoff configuration. No study was made of intermediate flap settings. Rotation velocity (V_R) and lift-off velocity (V_{LOF}) were chosen to optimize takeoff performance with all engines operating and with an engine failure. The optimization procedure and the effect of flap deflection are described in later sections.

The takeoff selected as a base case has:

$\delta_f = 41.1°$

T/W = .38

$\nu = 0$

V_R = 72 knots

Maximum angle of attack during rotation 12°

Elevator step -45°

The resulting takeoff performance, assuming a sea-level standard day and no wind or ground effects, is:

	All engines	Engine failure at V_1=72 knots
V_{LOF}	76.5 knots	76.1 knots
α_{LOF}	5.9°	8.2°
V_{35}	79.5 knots	77.4 knots
γ_{35}	8.6°	4.6°
Distance, 35 feet	1492 feet	1716 feet
R/C, 35 feet	1200 fpm	600 fpm

Takeoff field length is defined by reference 8 as the maximum of:

1) 1.15 x the all engine takeoff distance to a height of 35 feet
2) takeoff distance to 35 feet with one engine failure at V_1
3) rejected takeoff distance with decision at V_1

The required takeoff field length for the configuration above is 1716 feet, since 1.15 times the all-engine distance is 1716 feet, the engine-out distance is 1716 feet, and the corresponding rejected takeoff distance is 1666 feet. The three takeoff distances and some assumptions are shown schematically in figures 3a,b,c. A time history of distance, altitude, angle of attack, and velocity for the all engine and engine out cases is shown in figure 4.

The flight envelope for δ_f = 41.1, figure 5, shows the positions of the rotation, liftoff, and climbout velocities with respect to margin requirements and climb capabilities. Note the lack of constraint by minimum control speed as discussed earlier. The liftoff speeds are well above $V_{s_{3eng}}$ + 10; the engine out climbout speed is more than twenty knots above Vmin. It may be seen also that the engine out climb capability

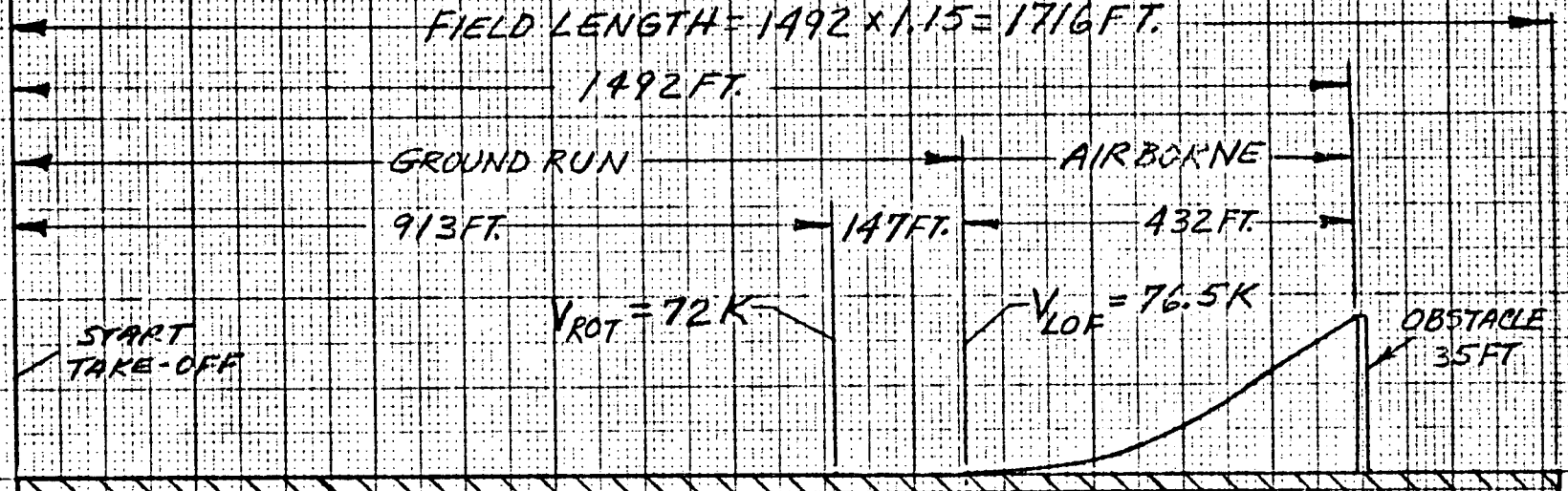

(a) FOUR ENGINES OPERATING, $\delta_f = 41.1°$, $T/W = 0.38$.

FIGURE 3.- TAKEOFF FIELD LENGTH.

NASA
AMES RESEARCH CENTER

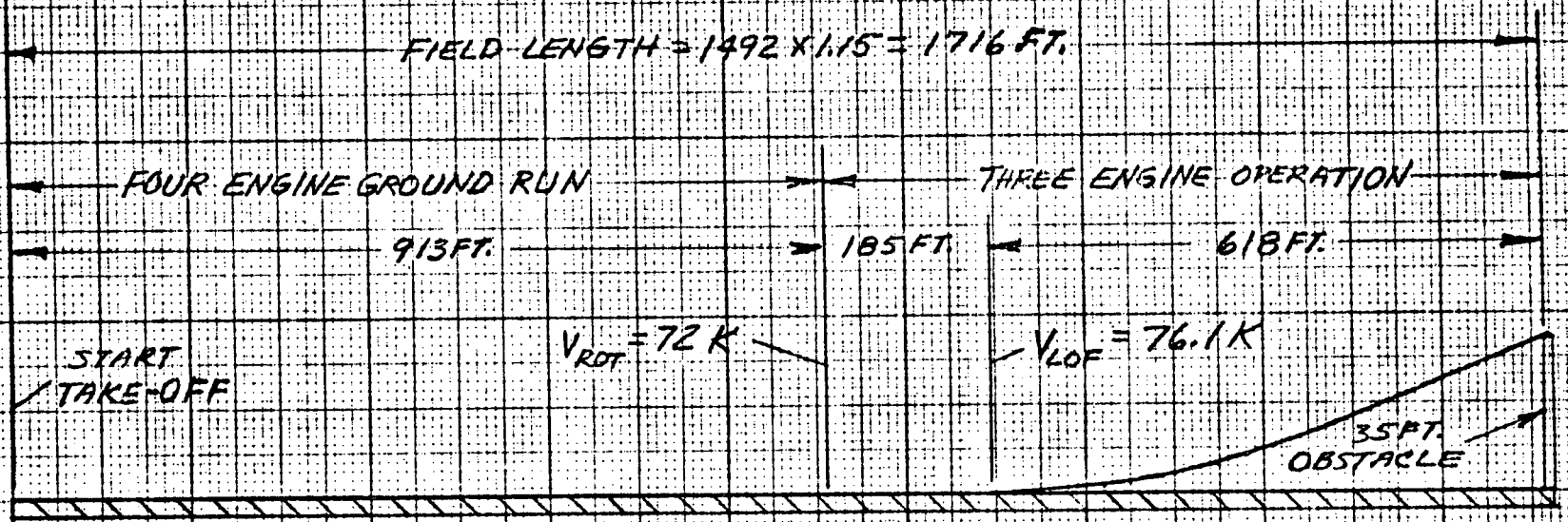

(b) CONTINUED TAKEOFF WITH ONE ENGINE INOPERATIVE, $\delta_f = 41.1°$; $T/W = 0.38$.
ENGINE FAILURE AT V_1 = 72 KT.
ENGINE WINDDOWN OVER 1 SEC.
NO POWER ADVANCEMENT

FIGURE 3. — CONTINUED.

NASA
AMES RESEARCH CENTER

(c) REJECTED TAKEOFF, $S_f = 41.1°$, $T/W = 0.38$.
ENGINE FAILURE AT $V_1 = 72$ KTS.
$\mu_B = 0.45$
LIFT DUMPED
TWO ENGINES REVERSED TO 40% THRUST
$\mu_R = 0.05$
MAX. DECELERATION = 0.516

FIGURE 3.- CONCLUDED.

NASA
AMES RESEARCH CENTER

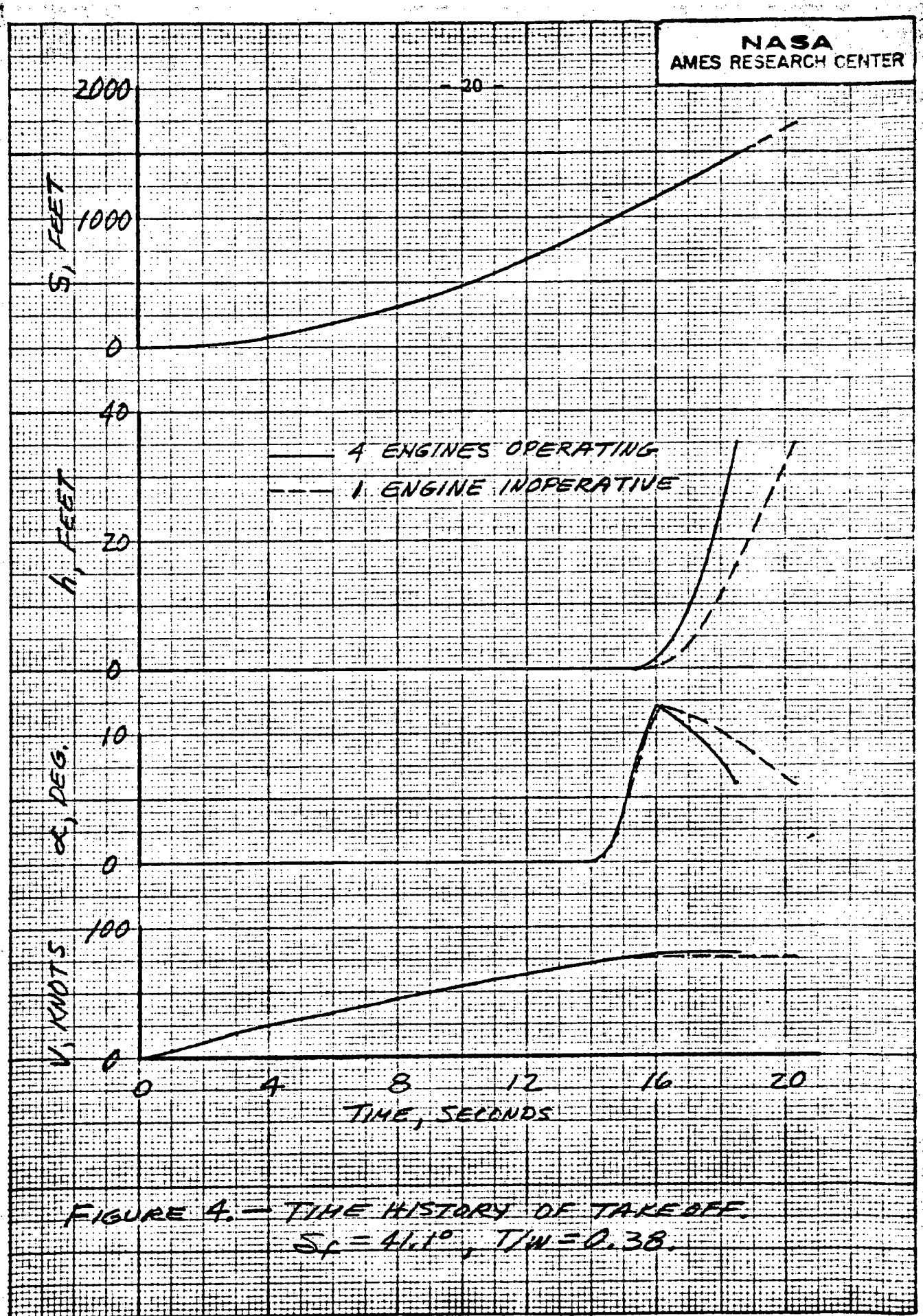

FIGURE 4.— TIME HISTORY OF TAKEOFF.
$\delta_f = 41.1°$, $T/W = 0.38$.

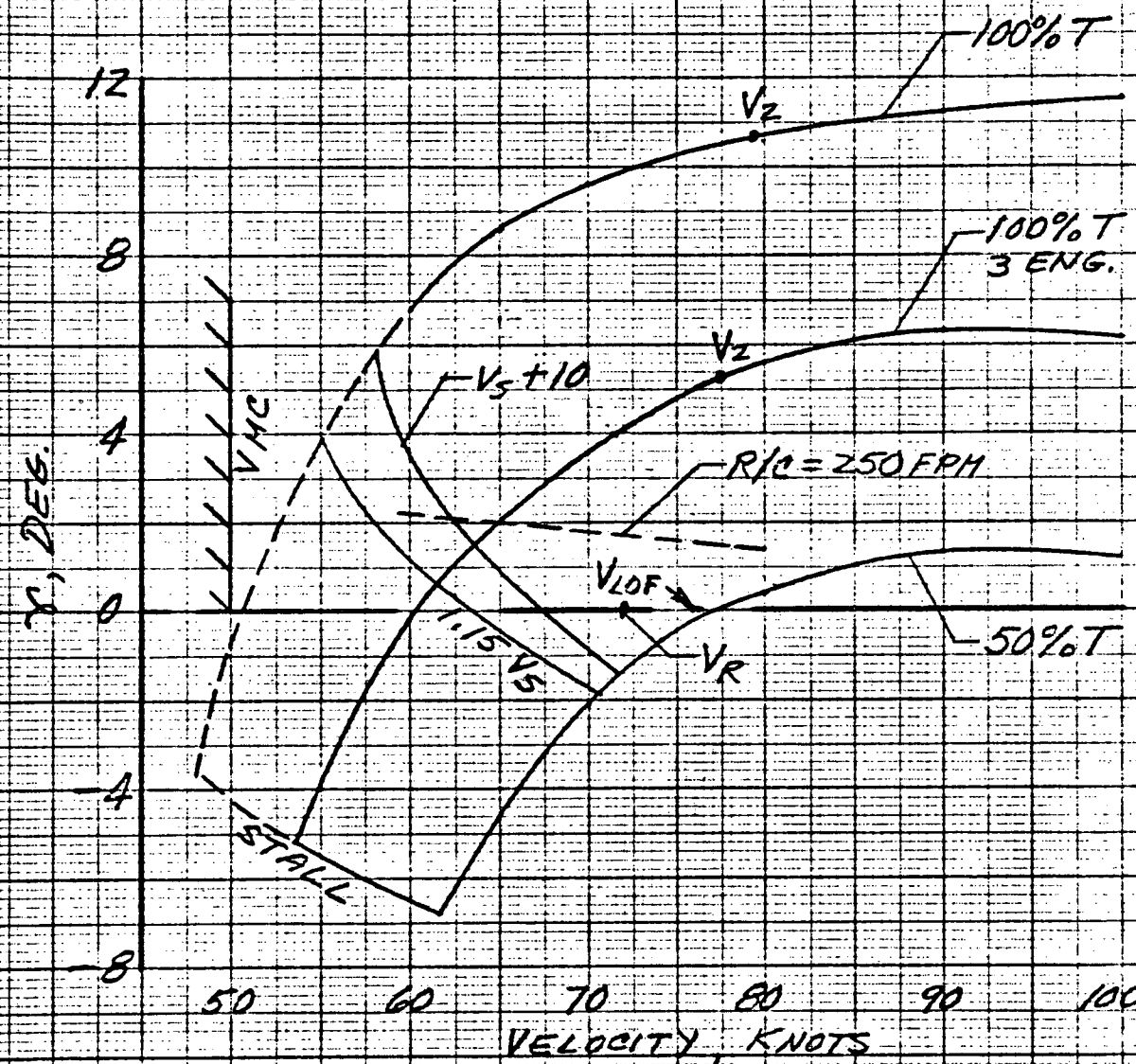

FIGURE 5.- TAKEOFF OPERATING ENVELOPE.
$\delta_f = 41.1$, $\gamma = 0°$, $T/W = 0.38$.

far exceeds the 250 fpm and 300 fpm requirements at V_{LOF} and V_2 respectively. The rate of climb available in unaccelerated flight at the lift-off speed, 76.1 knots, is 670 fpm. At 35 feet altitude the aircraft climbs at 600 fpm while accelerating .9ft/sec^2. The corresponding unaccelerated rate of climb would be about 700 fpm.

Optimization of Takeoff Parameters

At given flap deflection, thrust level and gross weight, there are several additional parameters affecting takeoff performance. They include velocity at start of rotation, maximum angle of attack used during rotation, elevator step, and hot gas thrust deflection. For purposes of this analysis, the hot thrust was not deflected for takeoff. The elevator input was taken as a step change -45°, held for a variable length of time, and a ramp return. The time period that the step was held was chosen by an iterative technique to accomplish rotation to the maximum commanded angle of attack and then usually reduced to 6° angle of attack, as illustrated in figure 4. This transition angle of attack was taken as a function of altitude, from the point of maximum rotation until reaching 35 feet. These assumptions made rotation velocity (V_R) and maximum commanded angle of attack (α_M) the key parameters.

In general, as α_M is increased, takeoff distance is decreased, but there is a limit to how far the airplane can be rotated. To avoid tail scraping and overly rapid change of pitch attitude, α_M was limited to 15°. Note that the angle of attack for stall is over 25°. Takeoff distance must, however, be balanced with required climbout velocity. If the

airplane is over-rotated, it tends to lose speed after liftoff, even with the gradual reduction of alpha through transition. This tendency to decelerate is more pronounced as rotation velocity is increased for the same α_M.

With the aerodynamics of this swept augmentor wing, a maximum commanded angle of attack of 12° at the 41.1° flap and 15° at the 31.8 ° flap were found most acceptable at all thrust levels dealt with. Figure 6 shows the effect of α_M on takeoff performance in the baseline 41.1° flap configuration. Note that at α_M = 15° distance is reduced, gamma increased, but the aircraft loses speed after liftoff with an engine failure, an unacceptable situation.

The second key parameter is the velocity at which rotation is initiated. There is a minimum velocity, V_{Rmin}, below which the elevator step taken cannot begin to lift the nose gear. Increasing V_R above this velocity increases the takeoff distance, when all engines are operating or with an engine failure prior to V_R. The V_R that optimizes the takeoff distance is based on three factors: (1) distance to 35 foot height with all engines operating, (2) distance to 35 foot height with an engine failed, and (3) rejected takeoff distance with an engine failed. Figure 7a shows the effect of V_R on the three factors for the base case (T/W = 0.38, δ_f = 41.1°, W = 48,000 pounds). Increasing V_R above the minimum value increases the takeoff distance with all engines operating. Assuming an engine failure at V_R, the engine out-takeoff distance is minimized by using a V_R a few knots above V_{Rmin} because the improved climb gradient at the higher velocity more than compensates for the increased ground roll. The critical decision point

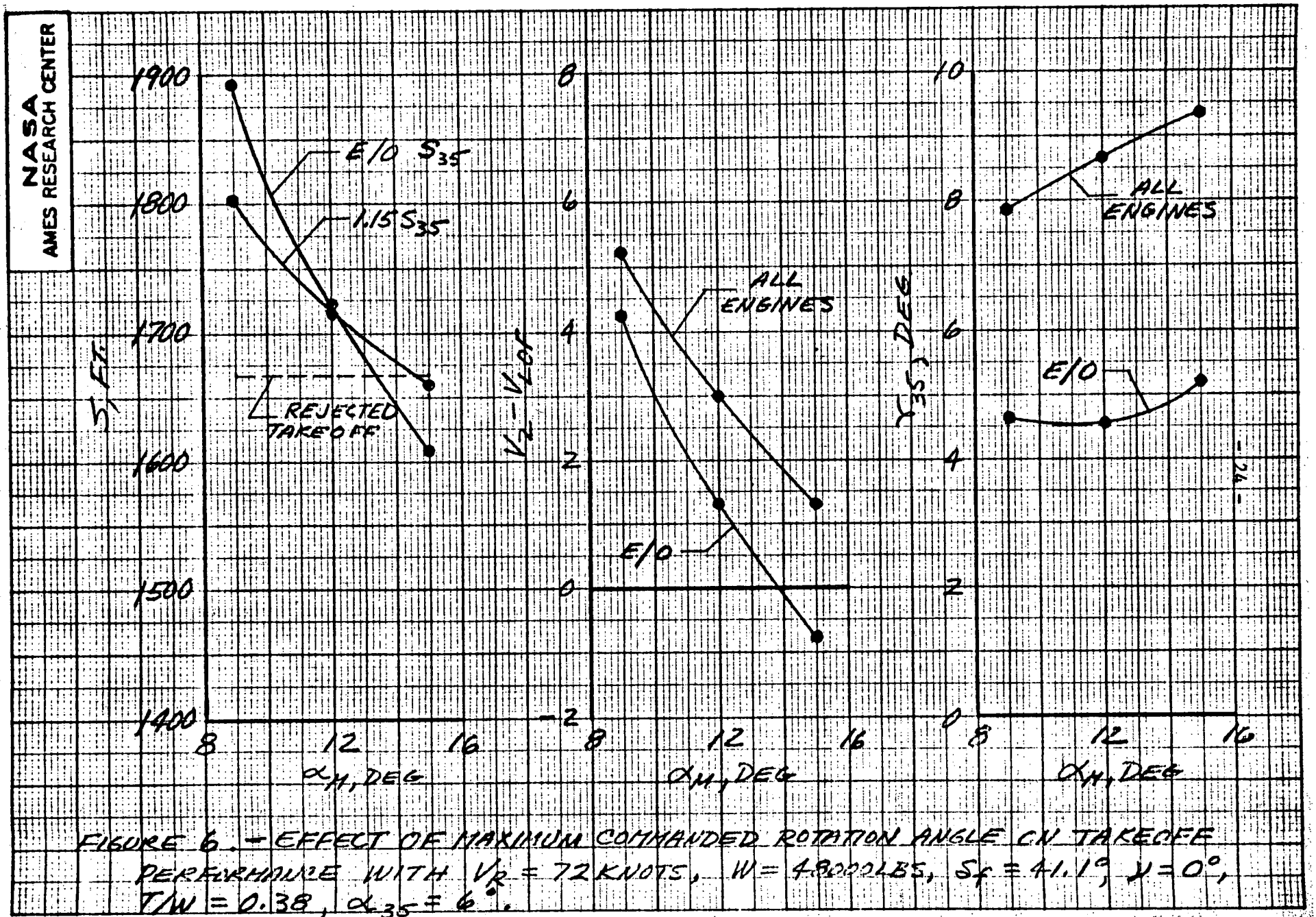

FIGURE 6. – EFFECT OF MAXIMUM COMMANDED ROTATION ANGLE ON TAKEOFF PERFORMANCE WITH V_R = 72 KNOTS, W = 48,000 LBS, S_f = 41.1°, ν = 0°, T/W = 0.38, α_{35} = 6°.

for a rejected takeoff, V_1, is at V_R because very effective braking has been assumed; therefore, the distance required to accelerate to V_1 and brake to a stop increases as V_R increases. Considering the three factors in selecting V_R, the minimum takeoff field length corresponds to the intersection of the E/O distance curve with the maximum of the rejected takeoff curve and 1.15 times the all engine curve. For the base case, the optimum value is a V_R = 72 knots and a field length of 1716 feet.

The effect of power on the selection of V_R and field length is illustrated in figures 7b and c by low and high power situations. These were obtained by varying the gross weight of the base aircraft. The intersection of the all engine and engine-out curves provides the minimum field length. However, it may be necessary or desirable to increase flight path angle by increasing V_R or to avoid deceleration by decreasing V_R. In the cases shown, rotation velocities of 76 knots and 68 knots were selected, resulting in slightly longer than minimum field length.

Flap and Thrust Effects

The effects of flap deflection and thrust level on takeoff field length are shown in figures 8 and 9. At the base thrust level, the reduction of flap deflection from 41.1° to 31.8° required an increase in rotation velocity to 80 knots, an increase in maximum alpha to 15° and a 200 foot increase in field length. At both flap settings it was found that when thrust was reduced about 13% (to T/W = .33), the required field length increased 300 to 350 feet. An equal increase in thrust had a lesser effect on field length, a decrease of 225 to 235 feet.

NASA
AMES RESEARCH CENTER

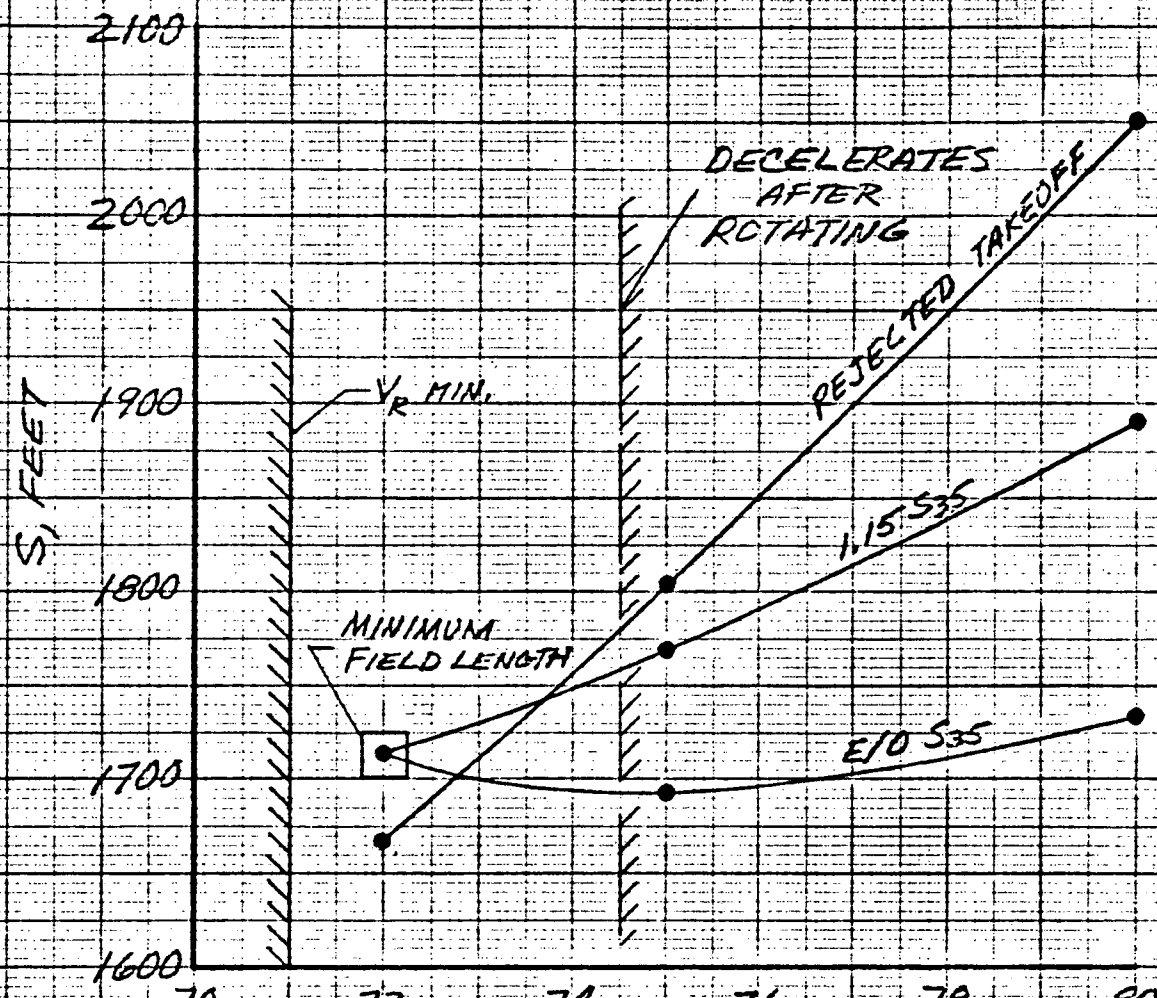

(a) BASE CASE
$W = 48000$ LBS. ($W/S = 80$ PSF)
$T/W = 0.38$

FIGURE 7.- EFFECT OF ROTATION VELOCITY ON TAKEOFF DISTANCE, $\delta_f = 41.1°$, $\alpha_H = 12°$.

NASA
AMES RESEARCH CENTER

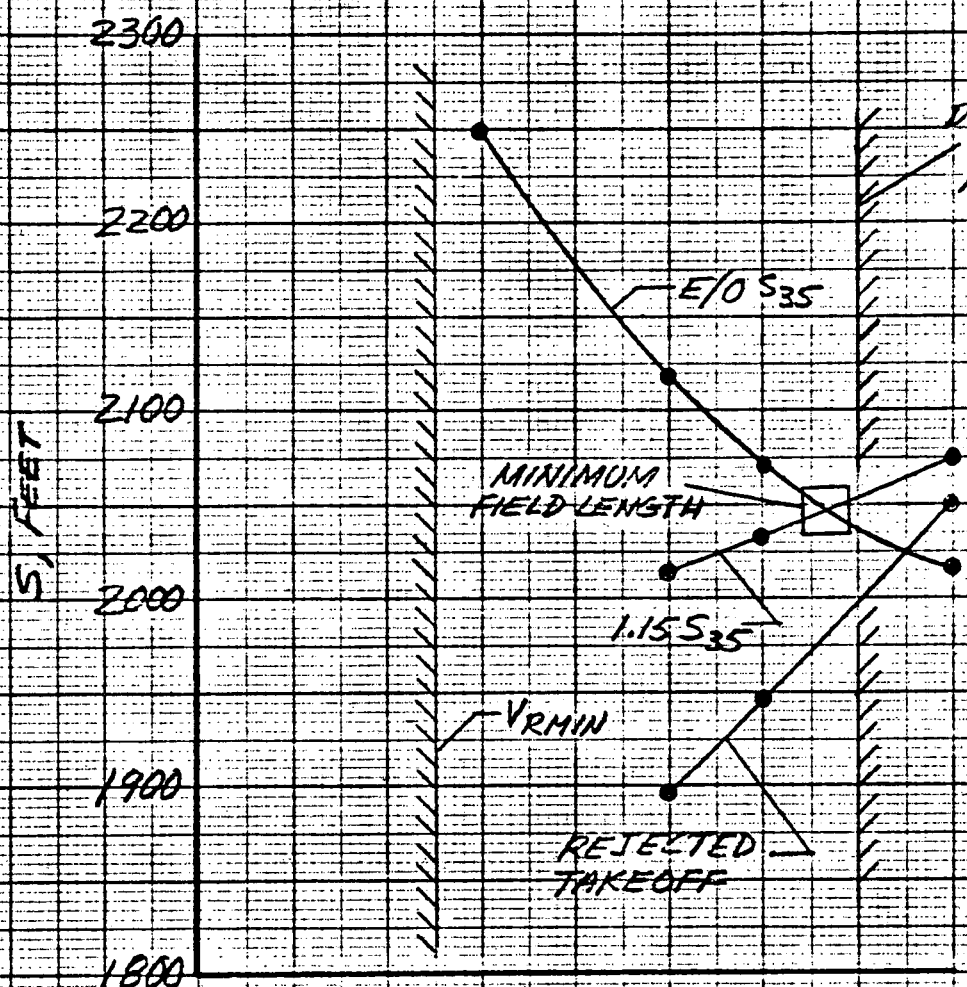

(b) LOW POWER
$W = 52000$ LBS ($W/S = 87$ PSF)
$T/W = 0.35$

FIGURE 7.- CONTINUED.

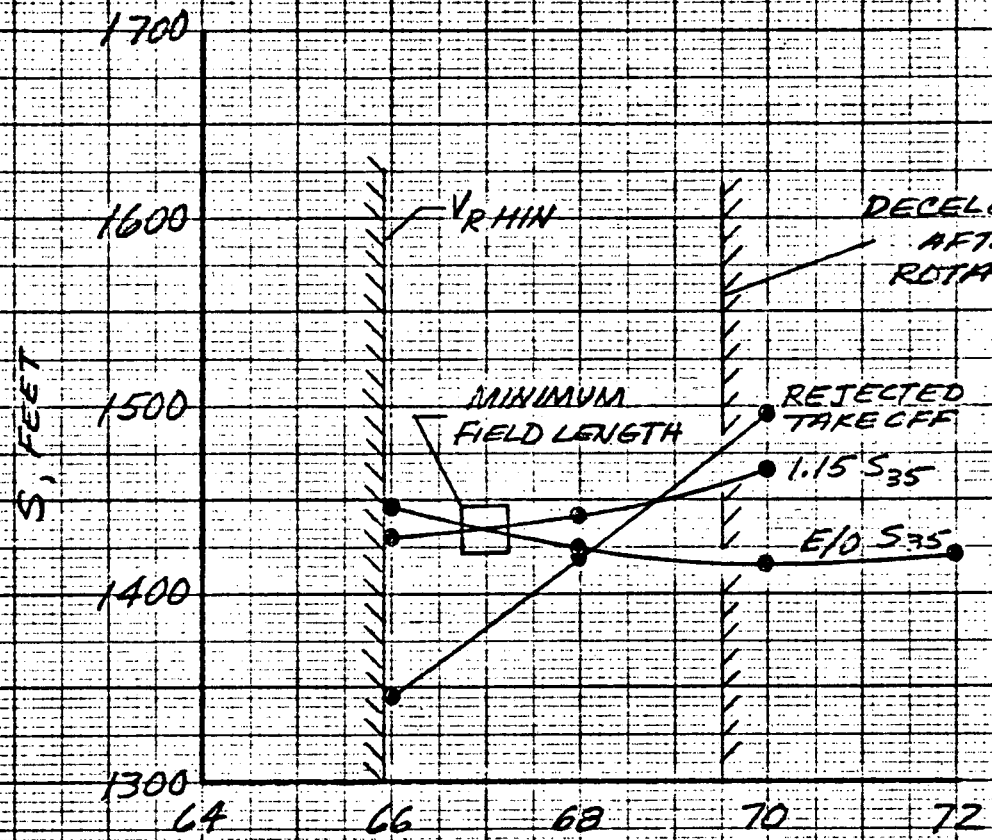

(C) HIGH POWER
$W = 44000$ LBS ($W/S = 73$ PSF)
$T/W = 0.415$

FIGURE 7.- CONCLUDED

NASA
AMES RESEARCH CENTER

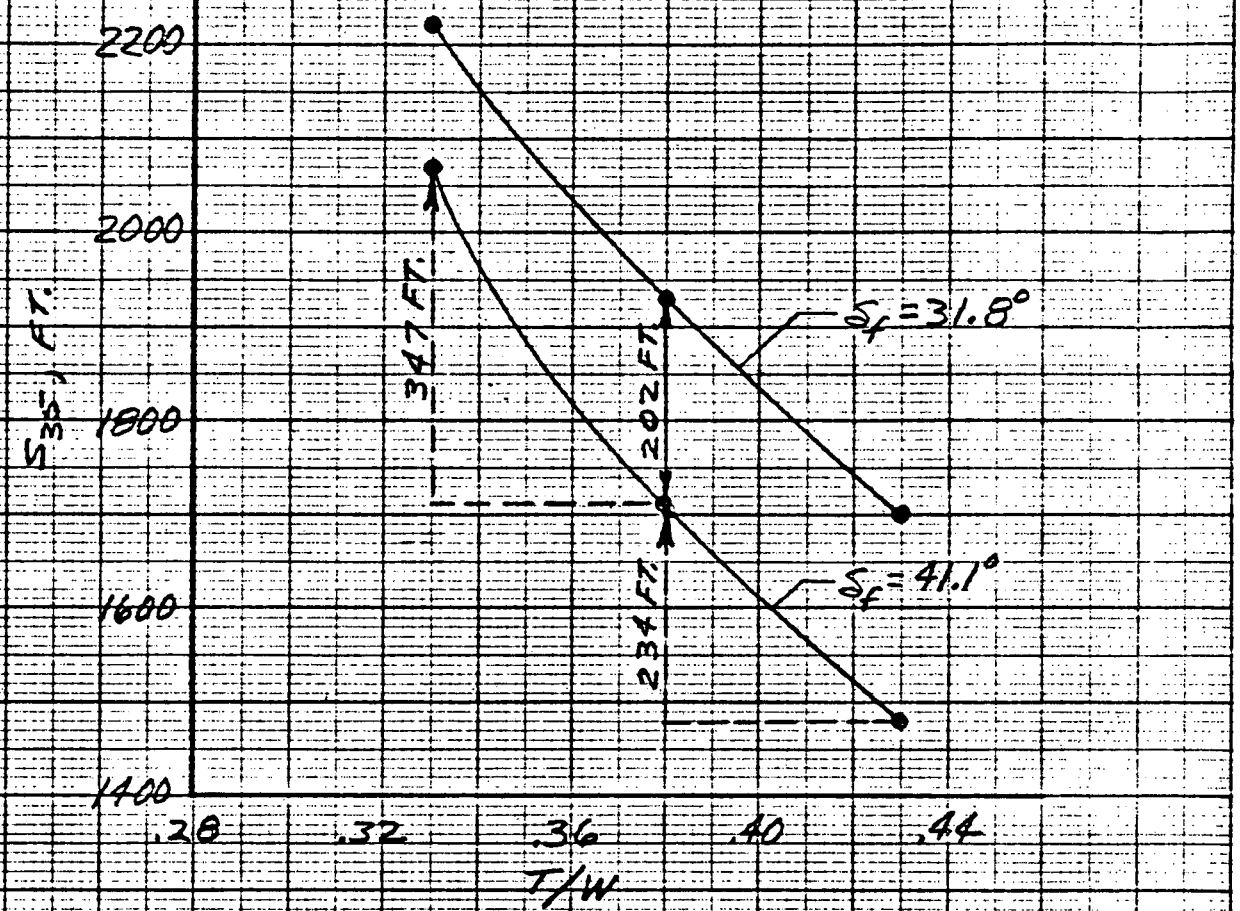

FIGURE 8 - EFFECT OF FLAP DEFLECTION AND T/W ON TAKEOFF FIELD LENGTH. W/S = 80 PSF.

NASA
AMES RESEARCH CENTER

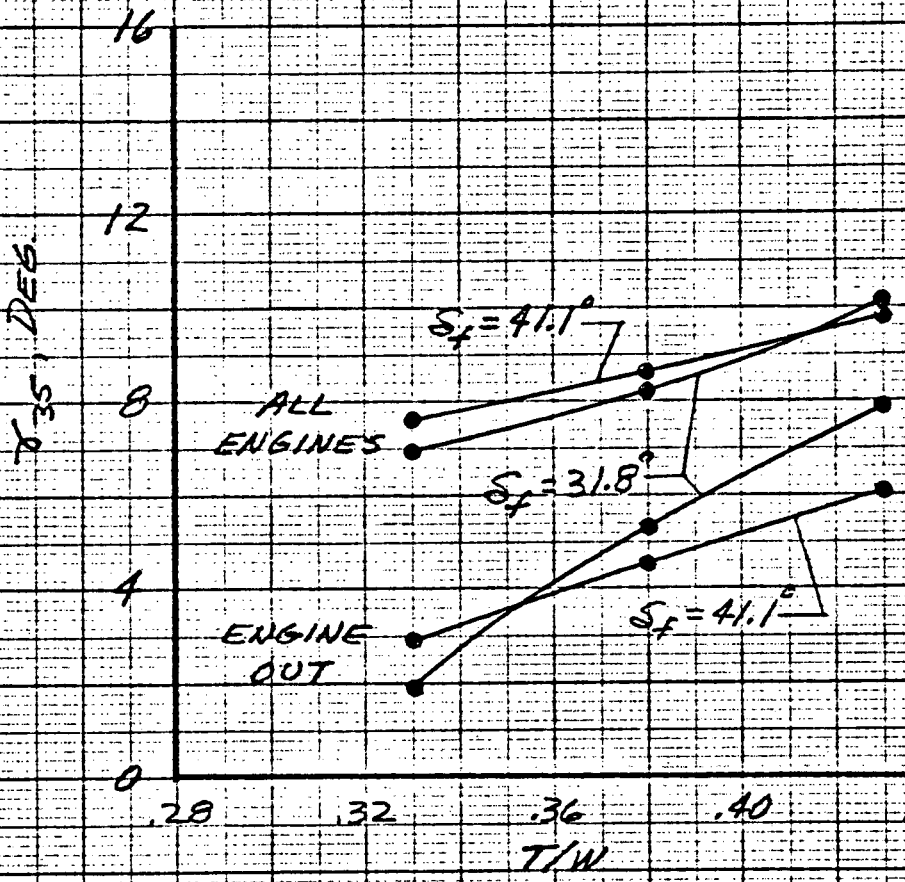

FIGURE 9.- EFFECT OF FLAP DEFLECTION AND T/W ON CLIMBOUT ANGLE. W/S = 80 PSF.

Flight path angle at 35 feet varies directly with thrust. The 13% thrust decrement reduces gamma about 1° with all engines, about 2° engine out. Flap deflection has little effect on the flight path angle, but rate of climb increases as the flap is reduced to 31.8° because velocity increases 9 to 10 knots.

The effects of flap and thrust on stall speeds and margins may be seen by comparing figures 10a and b. The stall speeds, and therefore the rotation speeds, are higher at the 31.8 flap. This increases the distance required for acceleration to liftoff speed and for braking from a rejected takeoff.

Effect of Gross Weight

A change in gross weight has a substantial effect on the required takeoff field length because there is an unfavorable effect due to both wing loading and thrust-to-weight ratio. Holding thrust at the baseline level and flap deflection at 41.1°, an increase in weight from 48,000 to 52,000 pounds resulted in a 350 feet increase in field length. A decrease from 48,000 to 44,000 pounds resulted in a 250 foot decrease. These distances are shown in figure 11. Optimizing these distances required changing the rotation speed from 72 knots to 76 knots in the 52,000 case, 68 knots in the 48,000. Rotation in each case was to an angle of attack of 12° dropping back to 6° by the time the 35 foot barrier is reached.

The increase in weight to 52,000 pounds resulted in a decrease of 1.6° in the flight path angle at 35 feet engine out (4.6° to 3.0°). The decreased weight resulted in an increase of 1.6° in gamma. The effects

NASA
AMES RESEARCH CENTER

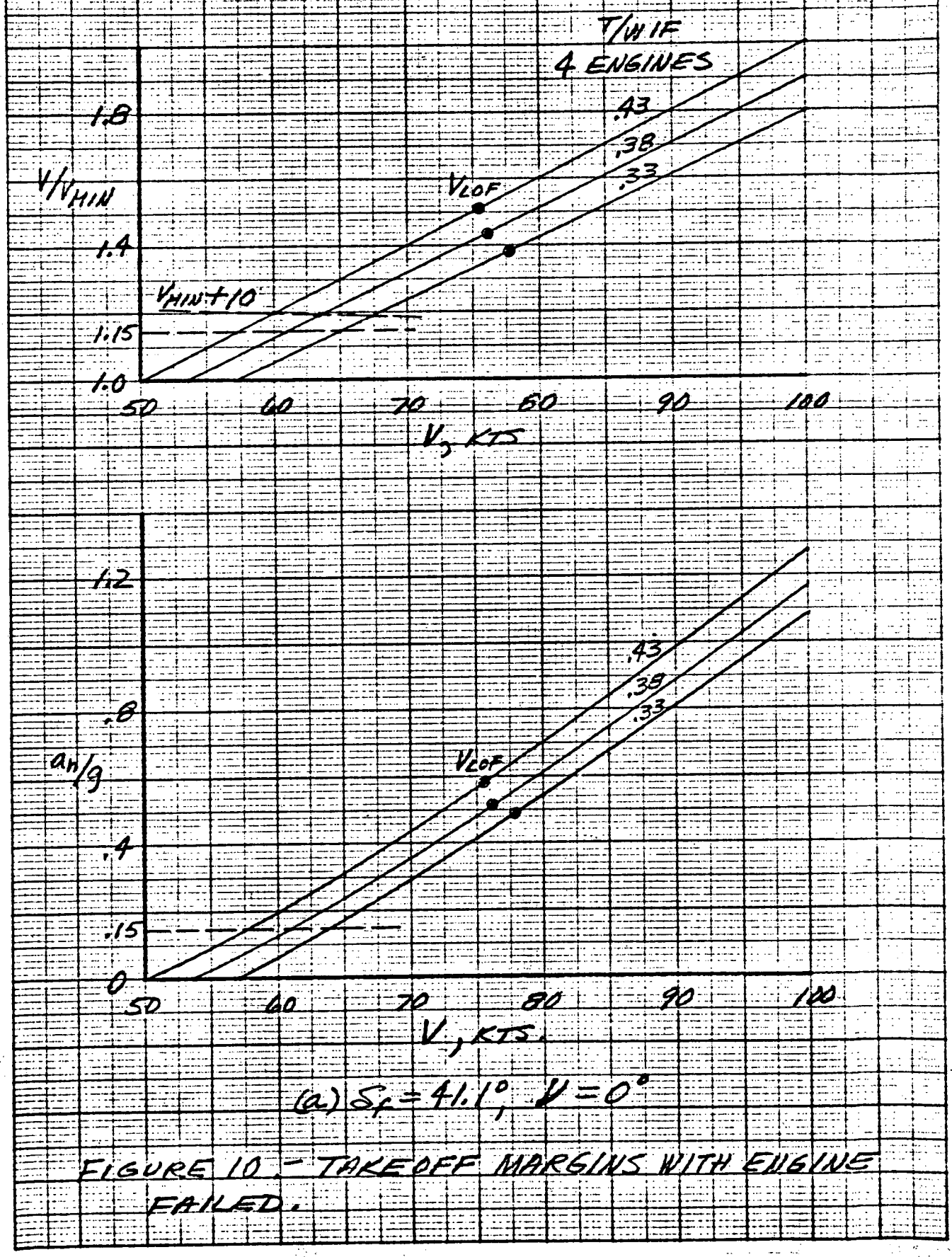

(a) $\delta_f = 41.1°$, $\gamma = 0°$

FIGURE 10 - TAKEOFF MARGINS WITH ENGINE FAILED.

NASA
AMES RESEARCH CENTER

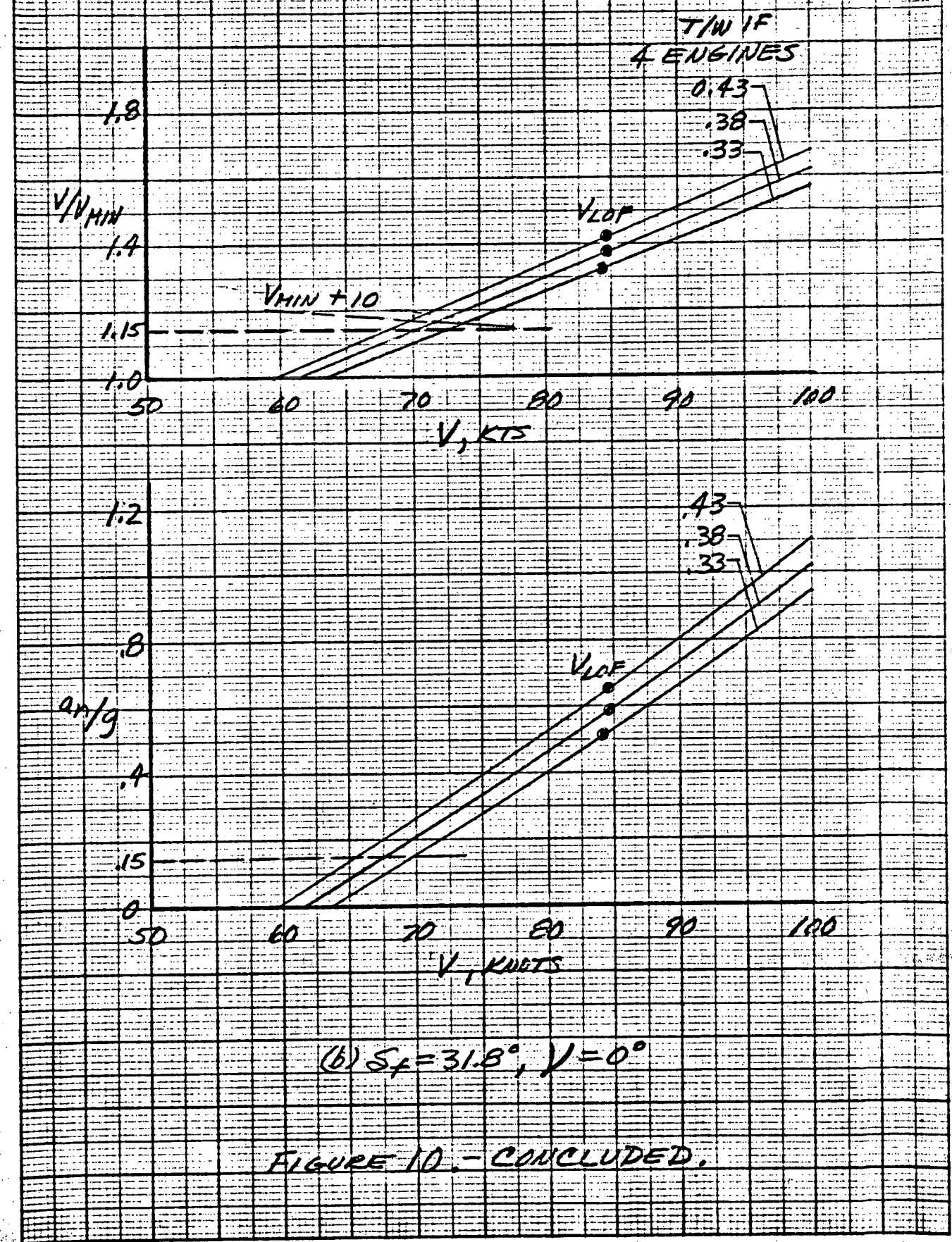

(b) $\delta_f = 31.8°$, $\gamma = 0°$

FIGURE 10.- CONCLUDED.

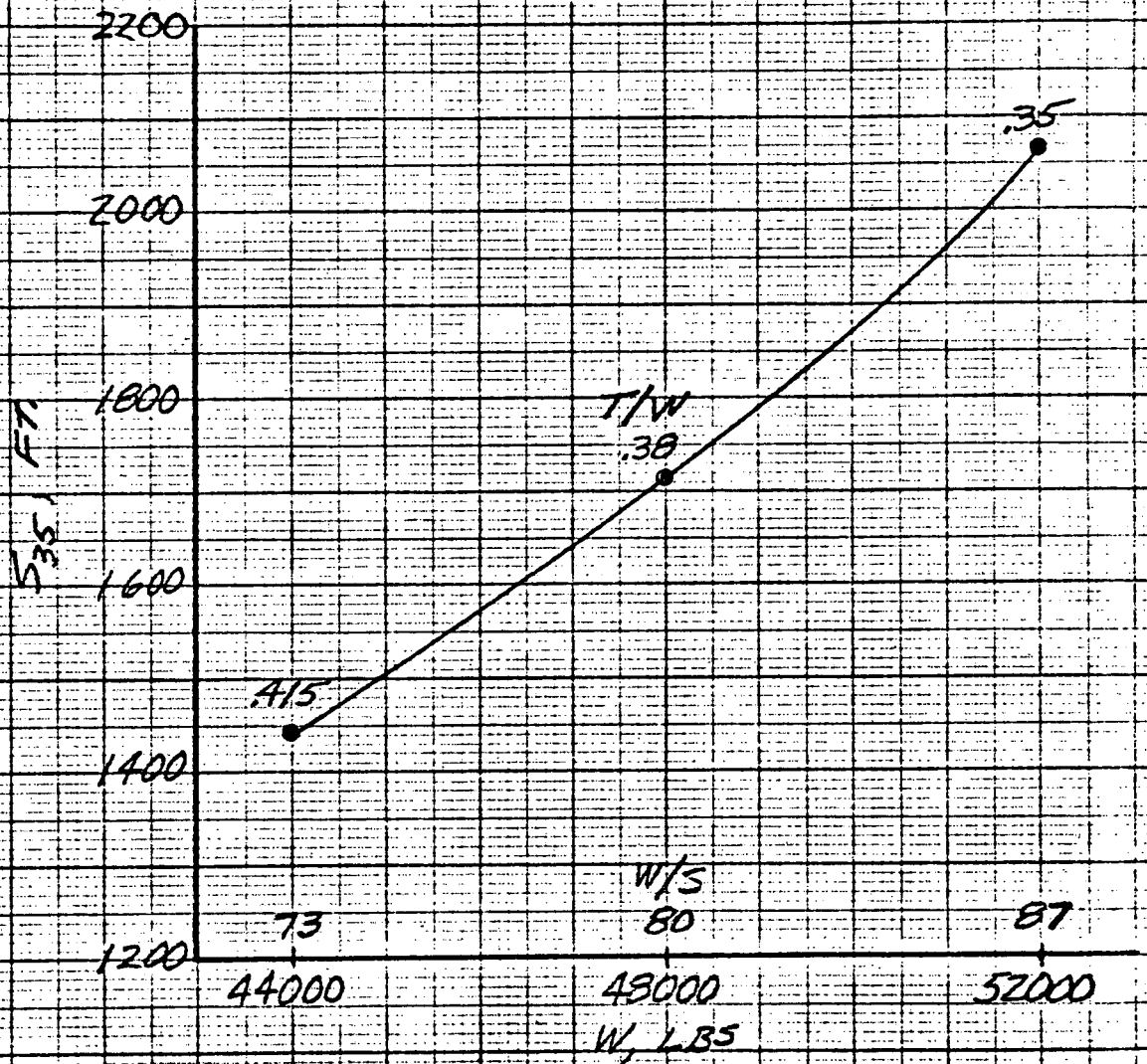

FIGURE 11.- EFFECT OF GROSS WEIGHT ON TAKEOFF FIELD LENGTH. $S_f = 41.1°$.

were similar in the corresponding all engine situations, 1.2° and 1.4°, respectively. If the two are compared on the basis of T/W, as in figure 12, it can be seen that the effect of weight change on takeoff field length is much larger than the corresponding effect of thrust change. This is because the wing loading is increased while the thrust-to-weight ratio is decreased.

Effect of Thrust Split

Some investigation was made of the effect of engine configuration on takeoff performance. A three-stream engine was simulated, maintaining the basic uninstalled thrust-to-weight ratio of 0.38. For this engine model, 37% of the thrust was used for wing flow. The 26% hot thrust and the other 37% cold thrust were exited directly aft during the takeoff maneuver. The duct and exit loss assumptions were the same as used for the two-stream engine analysis.

Takeoff field lengths were calculated at both 31.8° and 41.1° flap, and the 41.1° flap was found to require less distance, just as was found with the two-stream engine previously described. Comparing the best performance at T/W = .38, it was found that takeoff with the three-stream engine required about a 150 foot increase in field length over the two-stream configuration despite the allowing of rotation to 15° angle of attack with the three-stream engine. The climbout angles achieved with all engines operating and engine out were however only a fraction of a degree smaller with the three-stream. As can be seen in the following table, the main effects were the increased speed and rotation required for lift-off.

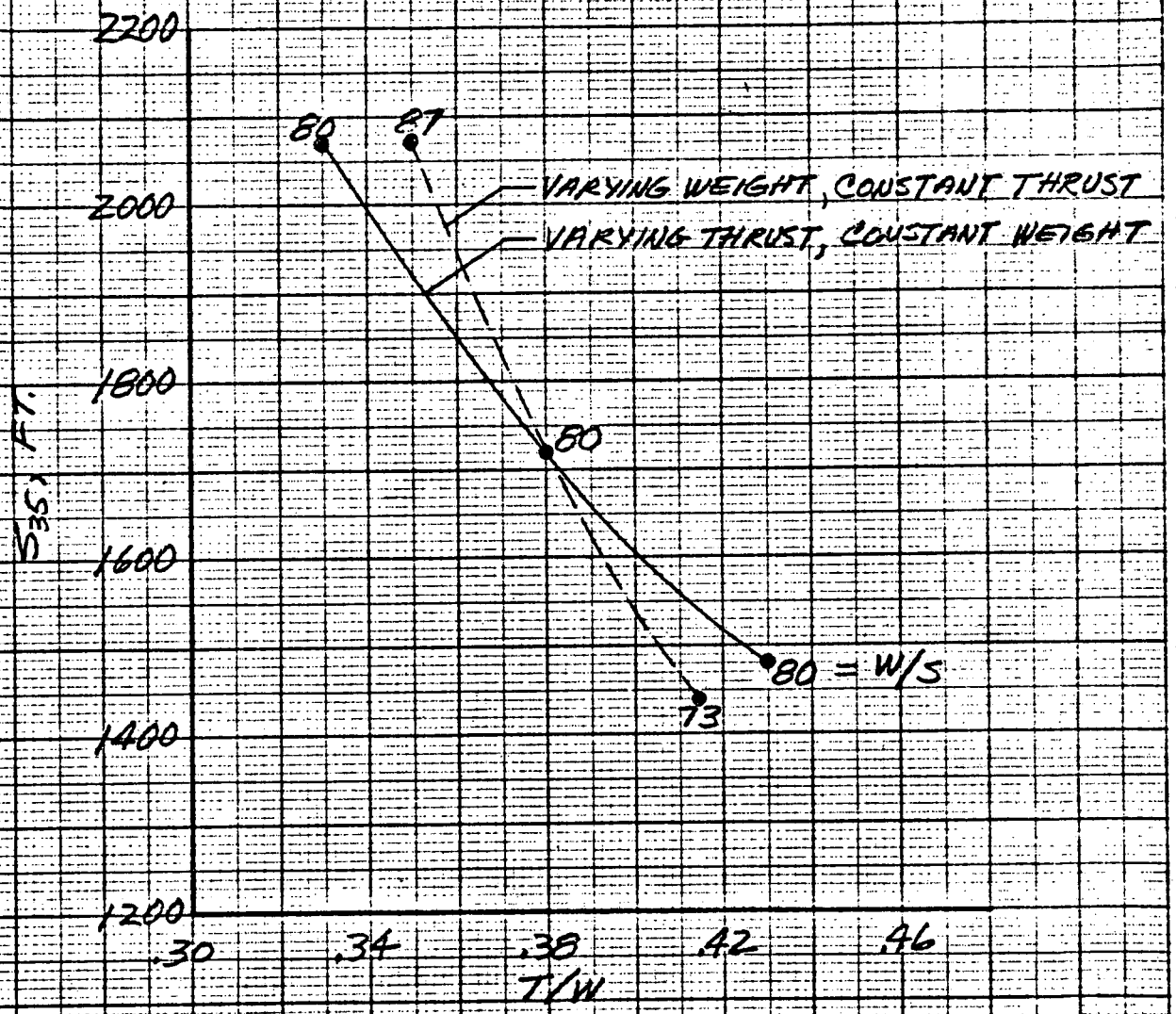

FIGURE 12.- EFFECT OF THRUST-WEIGHT RATIO ON TAKEOFF FIELD LENGTH.

All Engine Takeoff

	Three-stream	Two-stream
T/W	.38	.38
δ_f	41.1°	41.1°
ν	0°	0°
V_R	75 knots	72 knots
V_{LOF}	80.2 knots	76.5 knots
α_{LOF}	8.9°	5.9°
$\alpha_{max\ rot.}$	15°	12°
V_{35}	83.3 knots	79.5 knots
γ_{35}	8.2°	8.6°
S_{35}	1588 feet	1492 feet
1.15 S_{35}	1826 feet	1716 feet
Corresponding E/O S_{35}	1864 feet	1716 feet

The relation between performance with all engine operating and with engine failure at rotation was essentially the same for the three-stream engine as for the two-stream.

The effect of thrust-to-weight ratio and flap setting on takeoff field length are compared for the two engine configurations in figure 13. As may be seen, the field length is consistently larger for the three-stream engine, with the difference increasing as thrust is reduced. Differences in climbout angle between the engine configurations were found to be small at all flap and thrust settings considered.

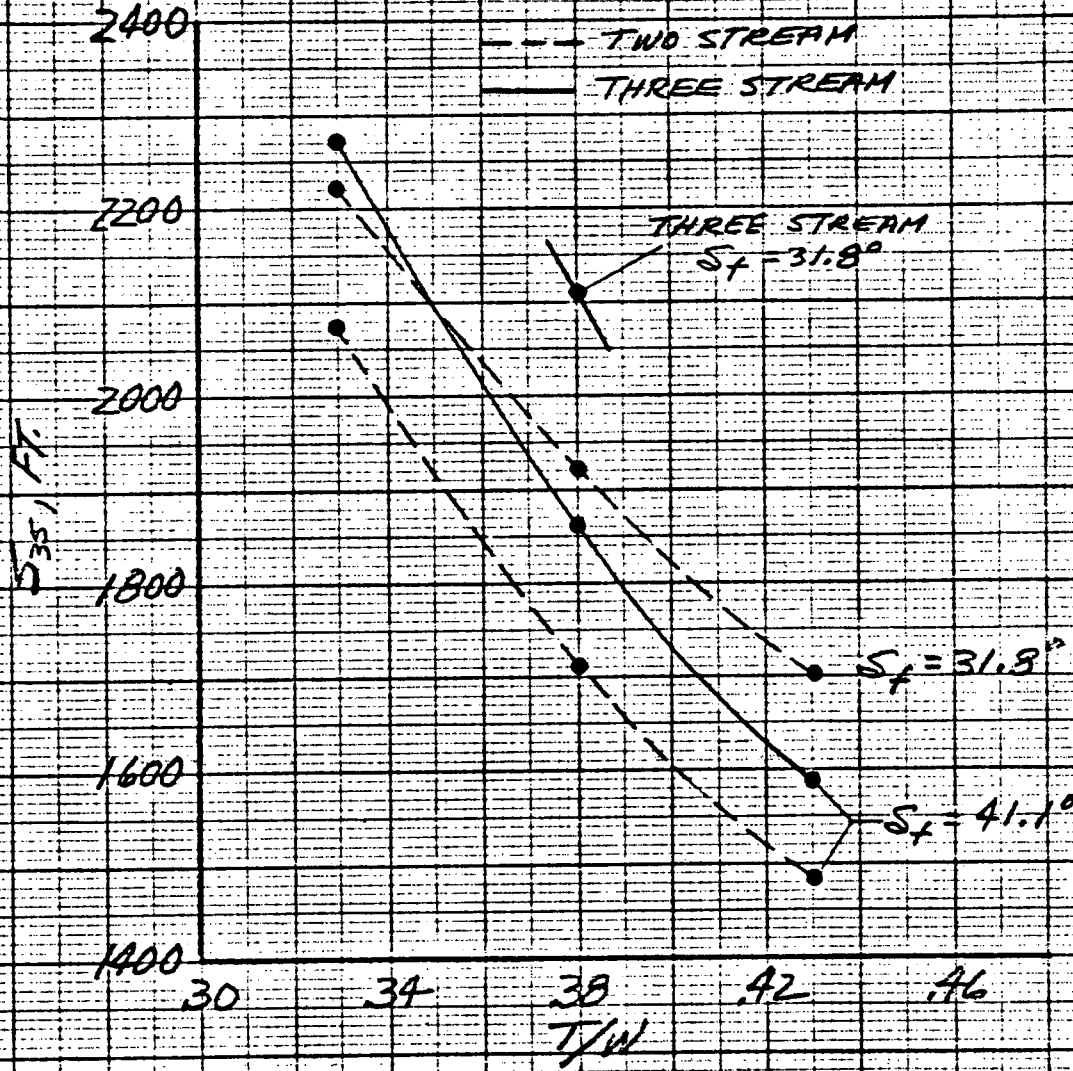

FIGURE 13. - COMPARISON OF TAKEOFF FIELD LENGTH FOR TWO AND THREE STREAM ENGINES, W/S = 80 PSF.

Approach and Landing

Approach and Landing Configuration Considerations

Aerodynamic data appropriate for approach and landing performance calculations is available at 51.1° and 70.6° flap deflections. Using this data the 70.6° flap and hot thrust deflection of 90° were found most appropriate to the relatively steep descent at low speed required for the final approach and landing configuration. The airspeed-flight path relations for this configuration are shown in figure 14. Interpolating between flap deflections, an intermediate flap setting of 55° and a higher velocity were found appropriate for earlier phases of the approach and for engine out waveoff. The deflection of the hot thrust from 90° to 0° or to 120° provides additional operational flexibility without a configuration change.

The nominal landing configuration was taken to be:

$\delta_f = 70.6°, \nu = 90°$

T/W = 0.2 (53% of takeoff power)

$\gamma = -7°$

V = 68 knots, $\alpha = 6.2°$

R/S = 840 fpm

The computed landing distance was 948 feet from a 35 foot height which results in a field length of 1580 feet if a 0.6 field length factor is applied. For this configuration the stall speed is about 57 knots at the landing power setting of 53% of thrust installed. It was noted earlier that the minimum control speed is well below the stall speeds for approach and landing configurations considered. Since sufficient longitudinal

NASA
AMES RESEARCH CENTER

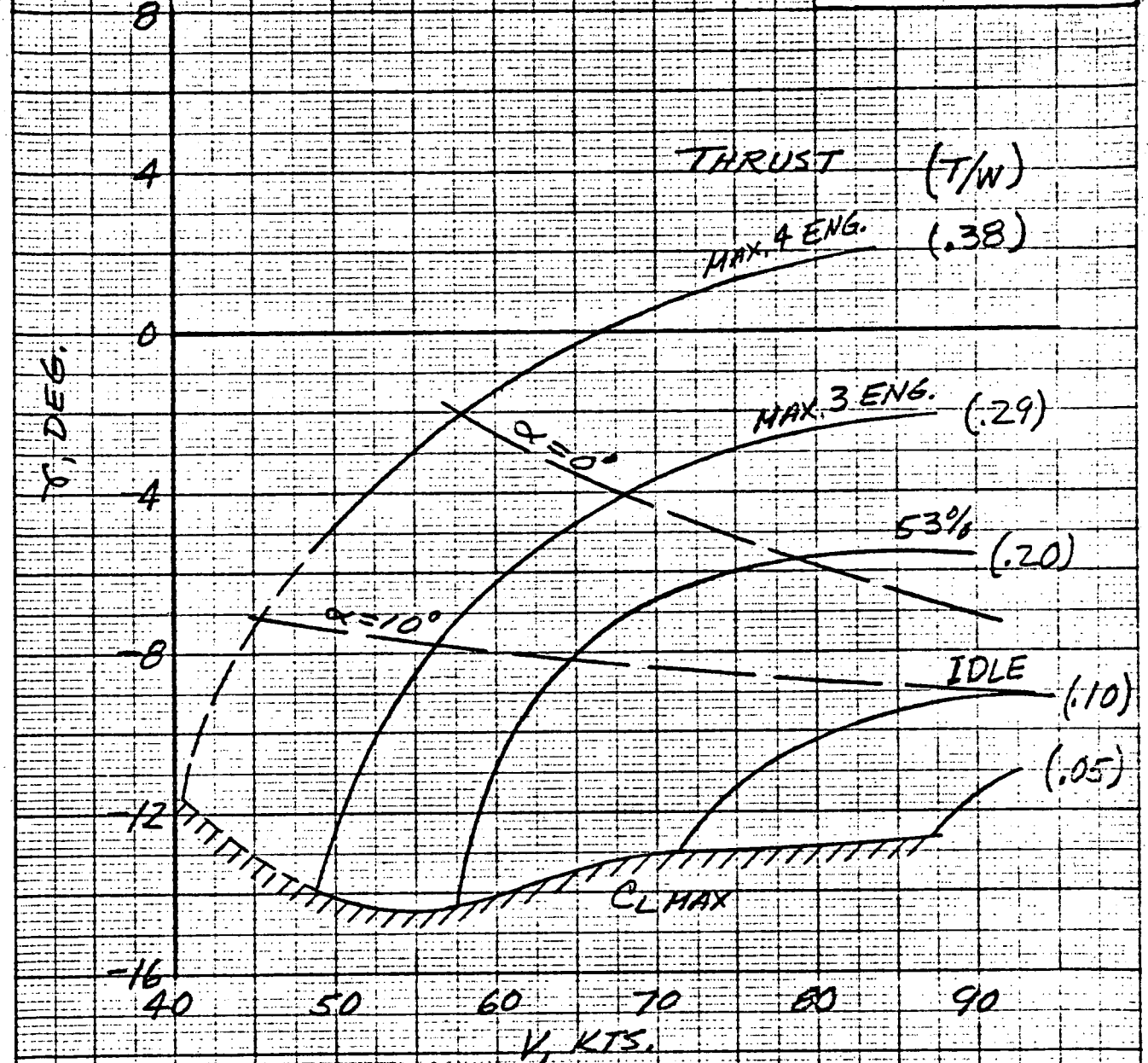

FIGURE 14.- LANDING CONFIGURATION ENVELOPE, $S_f = 70.6$, $\delta_a = 30°$, $\nu = 90°$, $i_t = -8.7$, $W/S = 80$ PSF.

control is available to achieve C_{Lmax}, the minimum speeds are synonymous with the stall speed.

In figure 15a the chosen landing speed is related to stall and maneuver margins and to flight path capabilities recommended in reference 7 for STOL aircraft. The stall margin represented by $1.15V_s$ was the lowest value recommended provided sufficient normal acceleration was available. The normal acceleration values shown in figure 15b exceed the levels recommended; therefore, it is felt that the 68 knot speed, slightly in excess of $1.15V_s$, is reasonable. Reference to figure 15c shows that applying full power at the chosen speed provides at least a level flight capability (rate of climb nearly 100 feet per minute). In order to satisfy the go-around climb requirement of 250 feet per minute (reference 8), it is necessary to change the hot gas deflection from 90° to 0°. This change increases the rate of climb to over 400 feet per minute with only a small increase in stall speed, figure 16.

While it is possible to maintain level flight with an engine out at 70.6° flap, (80 knots, $\nu = 0$) the waveoff climb requirement of reference 8 cannot be met. Flap deflection must be reduced to about 55° to make a 225 fpm rate of climb possible with an engine failed. The configuration to satisfy this requirement and to be on the chosen landing flight path at 7° is nominally referred to as an approach configuration, and it is defined as:

$\delta_f = 55°$, $\nu = 90°$

T/W = 0.12 (32% of thrust installed)

$\gamma = -7°$

V = 85 knots, $\alpha = 8.6$

R/S = 1040 fpm

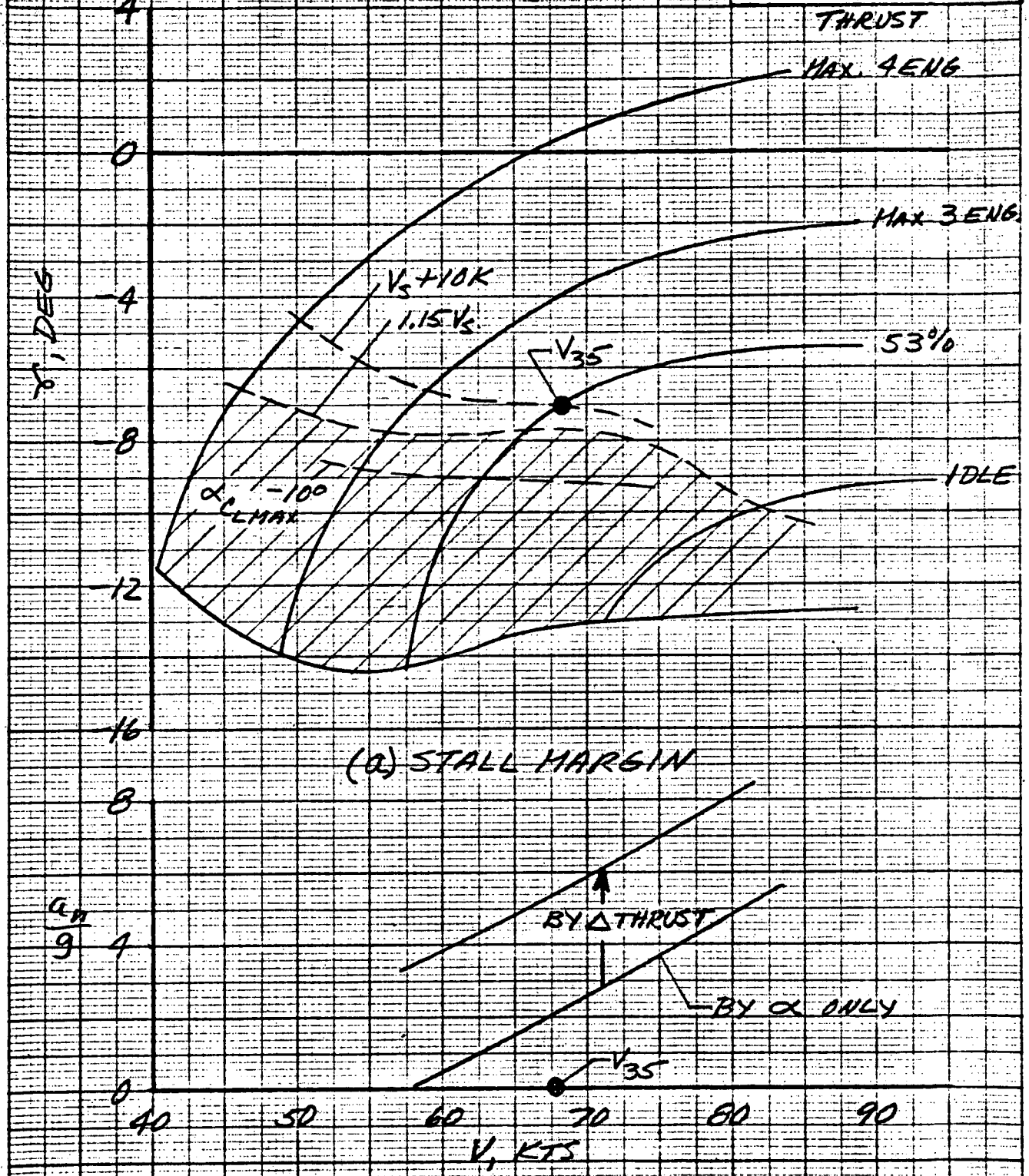

FIGURE 15.- MARGINS CONSIDERED FOR LANDING CONFIGURATION, $\delta_f = 70.6°$, $\delta_a = 30°$, $\mu = 90°$, $C_z = -8.7$, W/S = 80 PSF.

NASA
AMES RESEARCH CENTER

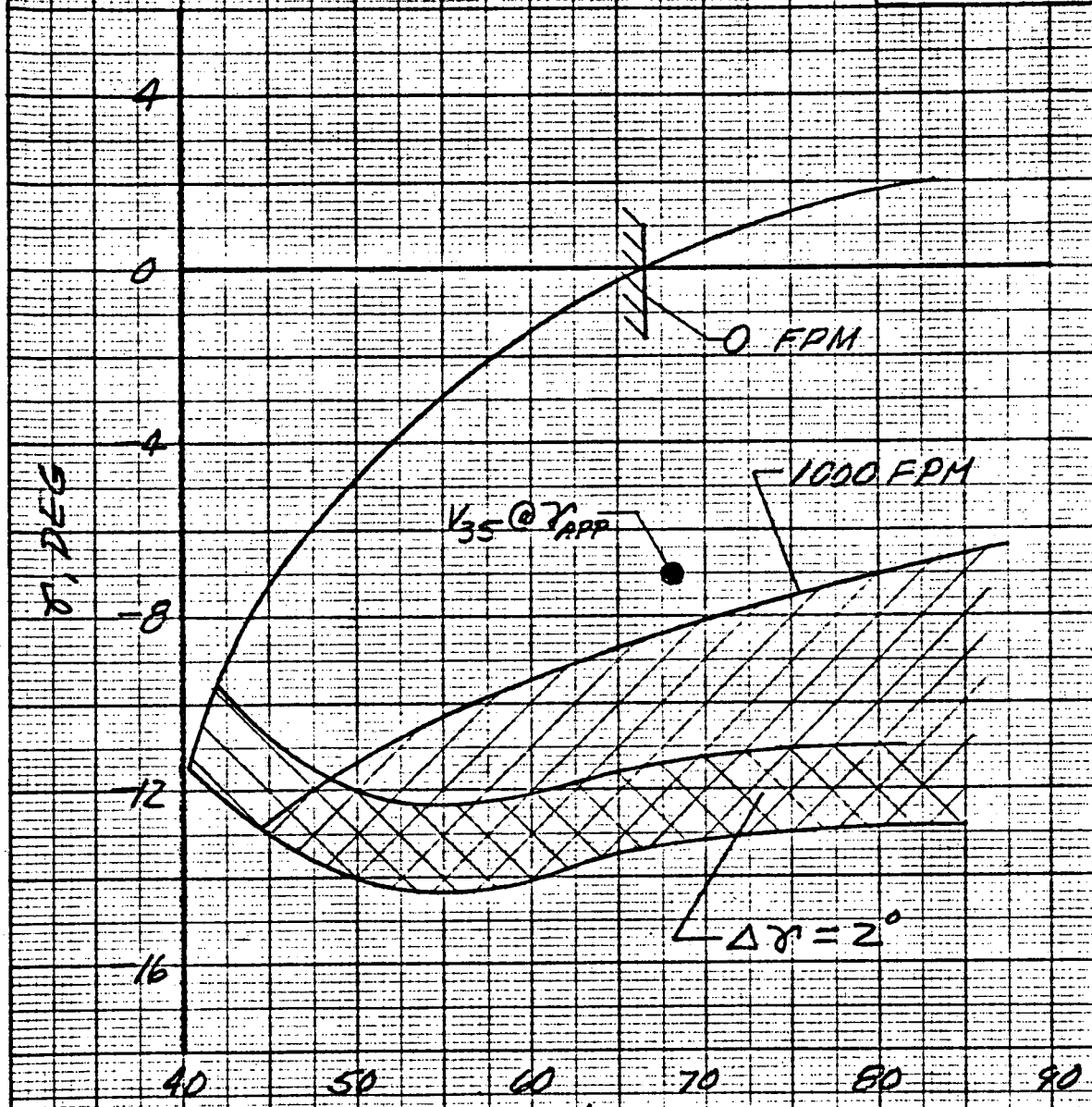

(a) FLIGHT PATH CAPABILITIES

FIGURE 15. - CONCLUDED.

NASA
AMES RESEARCH CENTER

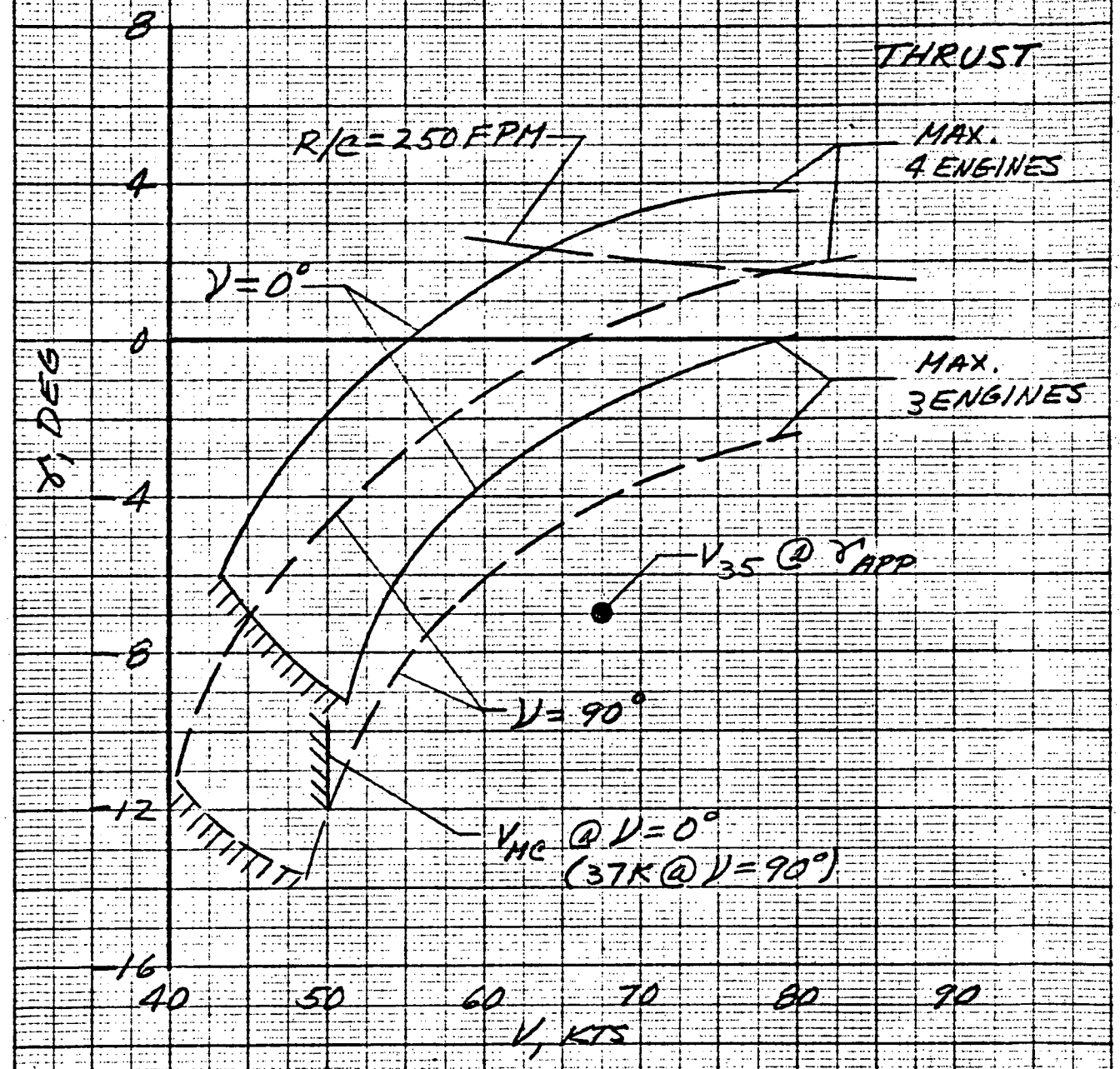

FIGURE 16.- EFFECT OF PRIMARY JET DEFLECTION IN LANDING CONFIGURATION. $\delta_f = 70.6°$, $\delta_a = 30°$, $i_t = -8.7$, W/S = 80 PSF.

At this flap setting, with three engines at full power and $\nu = 0$, the rate of climb is over 250 feet per minute (figure 17).

The three engine maximum power stall speed at 55° flap and $\nu = 90$ is 52.2 knots, which is 1.07 times the three engine maximum power stall speed for the landing flap configuration and satisfies the requirement of reference 8 that minimum speed in the approach configuration be not more than 1.10 minimum speed for the landing configuration. Likewise, at both approach and landing flap settings a change from $\nu = 90$ to $\nu = 0$ causes only a 5% increase in minimum speed. The approach configuration also satisfies the speed, maneuver and flight path margins used for the landing configuration.

Landing Performance

Figures 18 and 19 give a time history of the landing maneuver calculated to begin at a 35 feet altitude with the aircraft balanced and trimmed in the landing configuration. A partial flare to 13° angle of attack over two seconds ($d\theta/dt = 4.5°/sec$) and a 15% increase in thrust was employed to touch down at $h = -5.4$ fps at 64 knots. Landing distance, including braking at an average deceleration of .35g was 948 feet. Applying a 0.6 factor, landing field length was calculated to be 1580 feet. This is somewhat shorter than the takeoff field length of 1716 described earlier. Referring to figure 19, it can be seen that even though considerable rotation and some thrust increase were used, the normal acceleration was only 0.13g and the airspeed decreased 4 knots during the flare. This result occurs with STOL aircraft where a large portion of powered lift is utilized, and it is necessary to integrate the thrust and thrust deflection with

longitudinal control to augment the wing lift changes with angle of attack during the flare. A study of some of these characteristics and potential solutions for a similar aircraft is presented in reference 9.

NASA
AMES RESEARCH CENTER

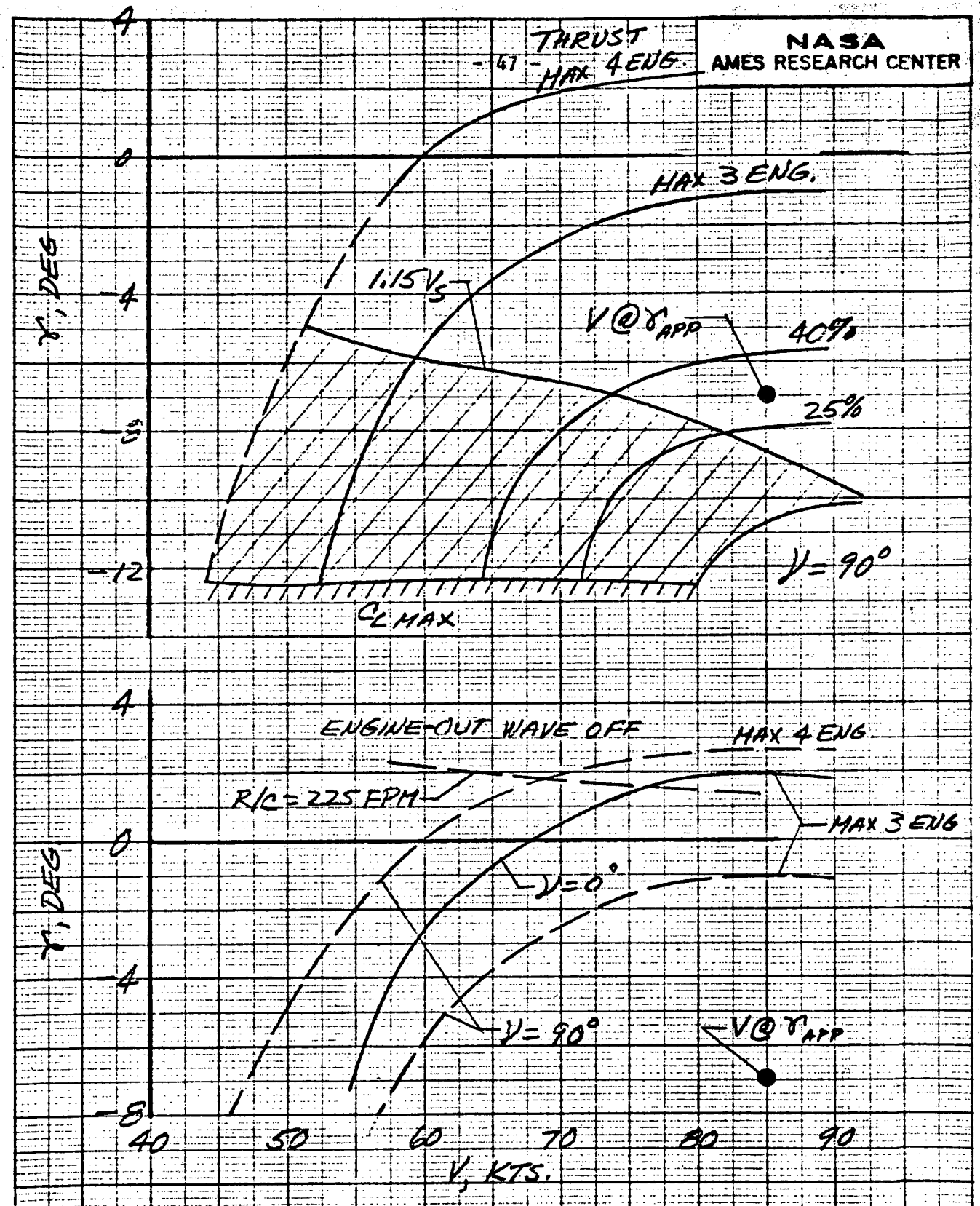

FIGURE 17.- APPROACH AND ENGINE-OUT WAVEOFF CONFIGURATION. $\delta_f = 55°$, $\delta_a = 30°$, $i_t = -8.7$, $W/S = 80$ PSF.

NASA
AMES RESEARCH CENTER

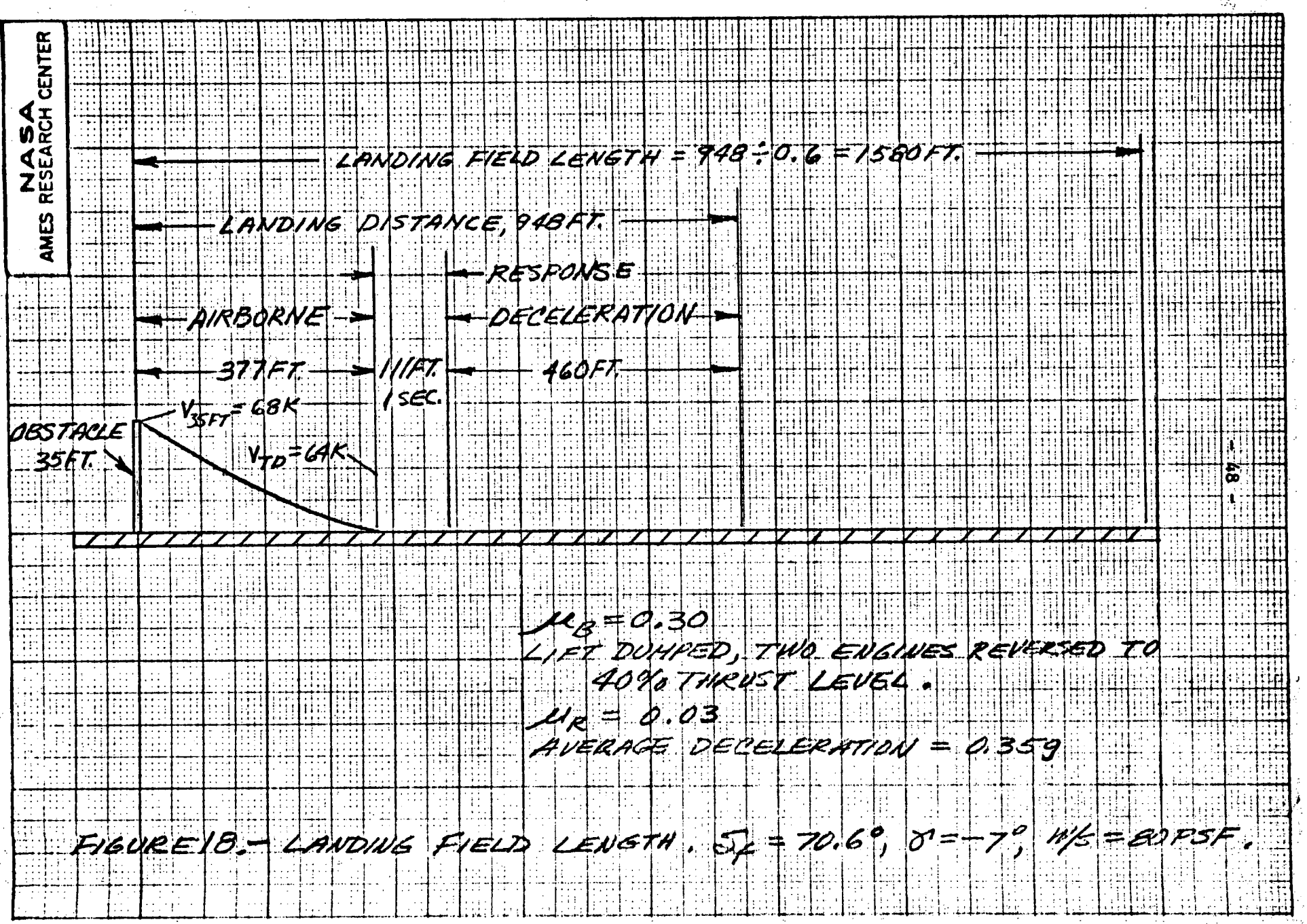

FIGURE 18.- LANDING FIELD LENGTH. $\Sigma_f = 70.6°$, $\gamma = -7°$, W/S = 80 PSF.

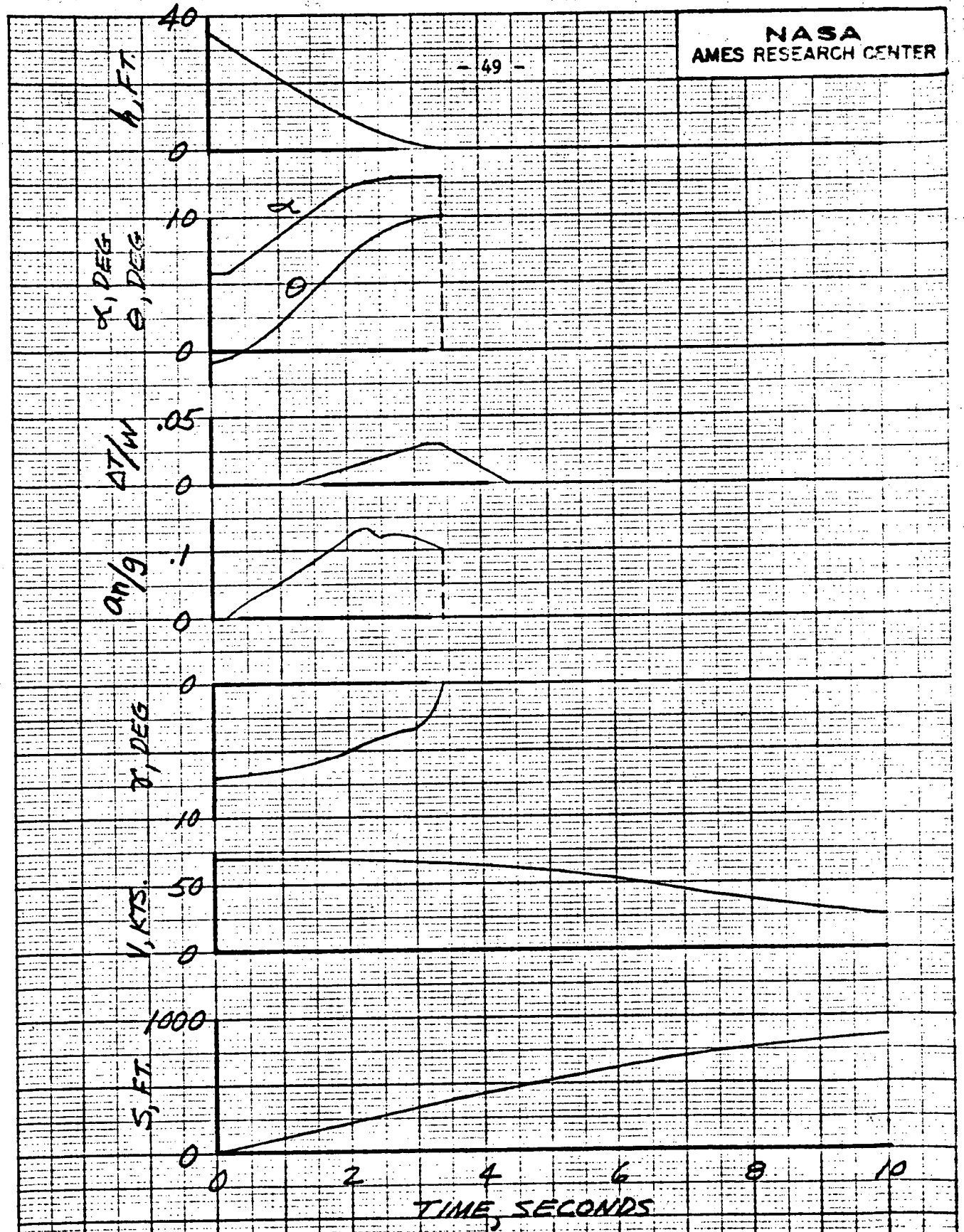

FIGURE 19.- TIME HISTORY OF LANDING FLARE, $\delta_{SA} = 70.6°$, $\delta_0 = 7°$, W/S = 80 PSF.

CONCLUSIONS

Assessment of the takeoff and landing performance of a swept augmentor wing airplane has shown that it could be operated in a STOL environment at a wing loading of 80 pounds per square foot and an uninstalled thrust-to-weight ratio of 0.38, in a configuration estimated to produce a noise level less than 90 PNdB. The required field length was found to be just over 1700 feet. It was shown that this performance could be achieved with satisfactory margins for control and safety.

The takeoff field length at T/W = 0.38 was calculated to be 1716 feet, equal to the engine out takeoff distance to 35 feet and 1.15 times the all engine distance. The climb capability in this case was about 9° all engines operating and 5° engine out. A 10% thrust change, at fixed weight and wing area, resulted in a 12% to 15% change in distance, reduction in thrust having the larger effect.

The landing analysis showed that the airplane could approach along a 7° glideslope at 68 knots. In that configuration a 950 foot landing could be made from 35 feet, resulting in a 1580 foot landing field length, based on a 0.6 field factor.

REFERENCES

1. Falarski, Michael D., and Koenig, David G. Aerodynamic Characteristics of a Large-Scale Model with a Swept Wing and Augmented Jet Flap. NASA TM X-62,029, July 1971.

2. O'Keefe, J. V., and Kelley G. S. Design Integration and Noise Studies for Jet STOL Aircraft, Volume I - Program Summary. NASA CR-114471, May 1972.

3. Roepcke, F. A., and Kelley, G. S. Design Integration and Noise Studies for Jet STOL Aircraft, Volume II - System Design and Evaluation Studies. NASA CR-114472, May 1972.

4. Campbell, J. M., Lawrence, R. L., and O'Keefe, J. V. Design Integration and Noise Studies for Jet STOL Aircraft, Volume III - Static Test Program. NASA CR-114473, May 1972.

5. Wang, T., Wright, F., and Mahal, A. Design Integration and Noise Studies for Jet STOL Aircraft, Volume IV - Wind Tunnel Test Program. NASA CR-114474, May 1972.

6. Falarski, Michael D., and Koenig, David G. Longitudinal and Lateral Stability and Control Characteristics of a Large-Scale Model with a Swept Wing and Augmented Jet Flap. NASA TM X-62,145, April 1972.

7. Innis, Robert C., Holzhauser, Curt A., and Quigley, Hervey C. Airworthiness Considerations for STOL Aircraft. NASA TN D-5594, January 1970.

8. Tentative Airworthiness Standards for Powered Lift Transport Category Aircraft. Flight Standards Service, Department of Transportation, Federal Aviation Administration. August 1970.

9. Franklin, James A., and Innis, Robert C. Longitudinal Handling Qualities During Approach and Landing of a Powered Lift STOL Aircraft. NASA TM X-62,144, March 1972.

10. Falarski, Michael D., and Koenig, David G. Longitudinal Aerodynamic Characteristics of a Large-Scale Model with a Swept Wing and Augmented Jet-Flap in Ground-Effect. NASA TMX-62,174. 1972.

APPENDIX A

Basic Aerodynamics

Figure A1. Lift, drag and moment characteristics with center of gravity at .35$\bar{c}$ horizontally and .20$\bar{c}$ below the wing chord, based on data of reference 1.

(a) Takeoff configuration; $\delta_f = 41.1°$, $i_T = -8.7°$

(b) Landing configuration; $\delta_f = 70.6°$, $i_T = -8.7°$

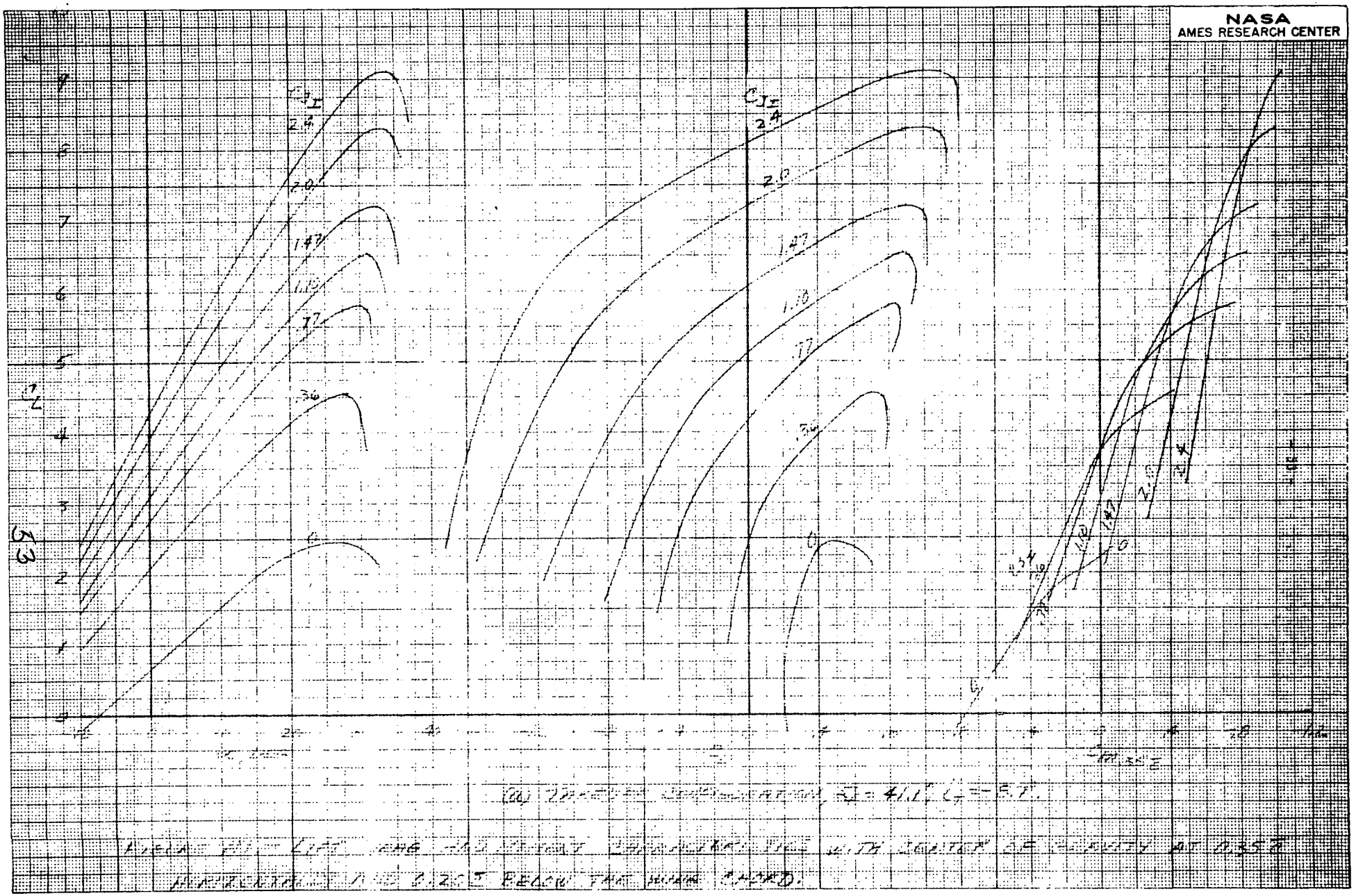

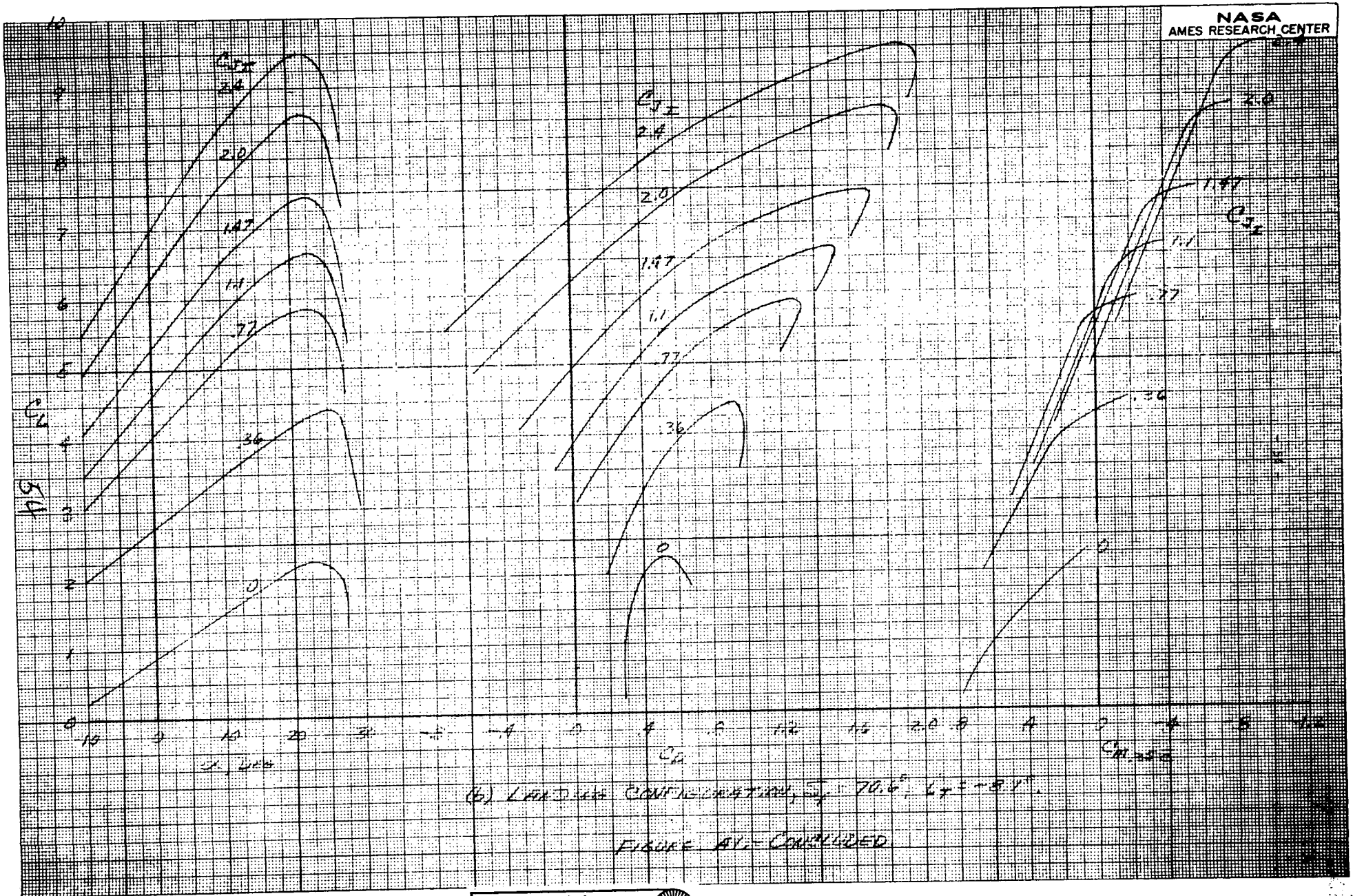

(b) LIFT-DRAG CHARACTERISTICS, $\delta_f = 70.4°$, $i_T = -8°$.

FIGURE 49.- CONCLUDED.

APPENDIX B

Computer Programs

Three computer programs were used in the performance analysis, a static trim program and dynamic takeoff and landing calculations. All are specifically structured for the powered-lift aircraft where aerodynamic lift, drag, and moment are functions of thrust level and velocity (C_J) as well as angle of attack and flap deflection. Only longitudinal calculations are handled.

Static Trim

The static trim program determines equilibrium flight conditions specified by angle of attack, flight path angle, thrust, thrust deflection, velocity, and flap deflection. Two of these and elevator are varied in an iterative procedure until the equilibrium point is reached. The stall speed associated with $C_{L_{max}}$ is also computed for each configuration. Engine out, temperature and altitude effects are also included.

Landing

The landing program has trim, landing and longitudinal maneuvering capabilities. The landing procedure is initiated by a trim calculation parallel to that in the static program. The dynamic model has two longitudinal degrees of freedom with the pitching moment equation being replaced by a command angle of attack. The landing roll computation includes delays, braking, thrust reversal, thrust change, and lift dumping. The

program was used for calculating rejected takeoff distance as well as landing performance.

Takeoff

The dynamic model used in the takeoff program has three degrees of freedom through the rotation maneuver, two thereafter. The rotation maneuver is defined by a rotation speed, commanded angle of attack (α_m), elevator step and elevator rate. Provided the elevator input and rotation speed are sufficient to lift the nose gear, the program iterates to find the time that the elevator step must be held to make $d\alpha/dt$ go to zero as α goes to α_m). For the transition phase from the point of maximum rotation to a point such as 35 feet, angle of attack is input as a function of altitude. From that point several modes of climbout are available, including constant theta, gamma, or velocity.

The program includes engine failure, gear lift, ground effect, and altitude effect capabilities.

APPENDIX C

As noted earlier, the primary basis of the data used is reference 1, data for a large-scale, swept-wing model out of ground effect and without a wing mounted propulsion system. Static tests showed that the augmentation ratio was lower than reported in other experiments, and therefore it was assumed for this analysis that the same aerodynamics could be achieved with an isentropic thrust coefficient reduced by $\frac{1.1}{1.25}$. These assumed characteristics are compared in figure C1 with data obtained in reference 6, the same model but with a different diffuser angle. Even though it appears that the assumption was valid, it should be pointed out that there was little difference in static augmentation measured in these two tests. Additional static and wind tunnel tests and analyses of augmentor wing characteristics are contained in references 4 and 5. It appears that with the information presently available it is not possible to confidently relate static changes in augmentation with the aerodynamics at takeoff and landing speeds.

The same model of reference 6 was recently tested in ground effect and with propulsion systems mounted on the wing (reference 10). Representative characteristics are shown in figure C2 for a takeoff and a landing configuration. The data at an $h/\bar{c}$ of 2.04 correspond to the aircraft five feet above the ground level; whereas, an $h/\bar{c}$ of 1.34 would be two feet lower than normal ground position. Referring to the takeoff configuration (figure C1(a)), it is seen that in general ground proximity, with or without

wing mounted engines, improved lift and accelerating force. The maximum lift coefficient was not reached at the maximum angle of attack that could be tested near the ground, 18° at an $h/\bar{c}$ of 2.04 and 8° at an $h/\bar{c}$ of 1.34. The use of these data would result in a shorter takeoff distance than presented. Corresponding data for the landing configuration without wing mounted engines (figure C2(b)) showed little change in lift and drag when the ground was approached. At an $h/\bar{c}$ of 2.04, addition of the engines with thrust deflected downward had little effect for a thrust split with more hot gas than that of the configuration of this study. The addition of four wing mounted engines reduced the lift five to ten percent and reduced the drag. Maximum lift coefficient was not reached at 18°, the maximum angle of attack that could be tested. The effect of these data on the landing performance has not been determined. If the lift loss is primarily due to wing mounted engines, an increased approach speed, angle of attack, or flap deflection would be required. If it is primarily due to ground proximity, it will be necessary to compensate for the increased vertical velocity near the ground.

NASA
AMES RESEARCH CENTER

FIGURE 11 - EFFECT OF SWEPT AND UNSWEPT WING PLANFORM, TAKE-OFF CONFIGURATION, TAIL ON.

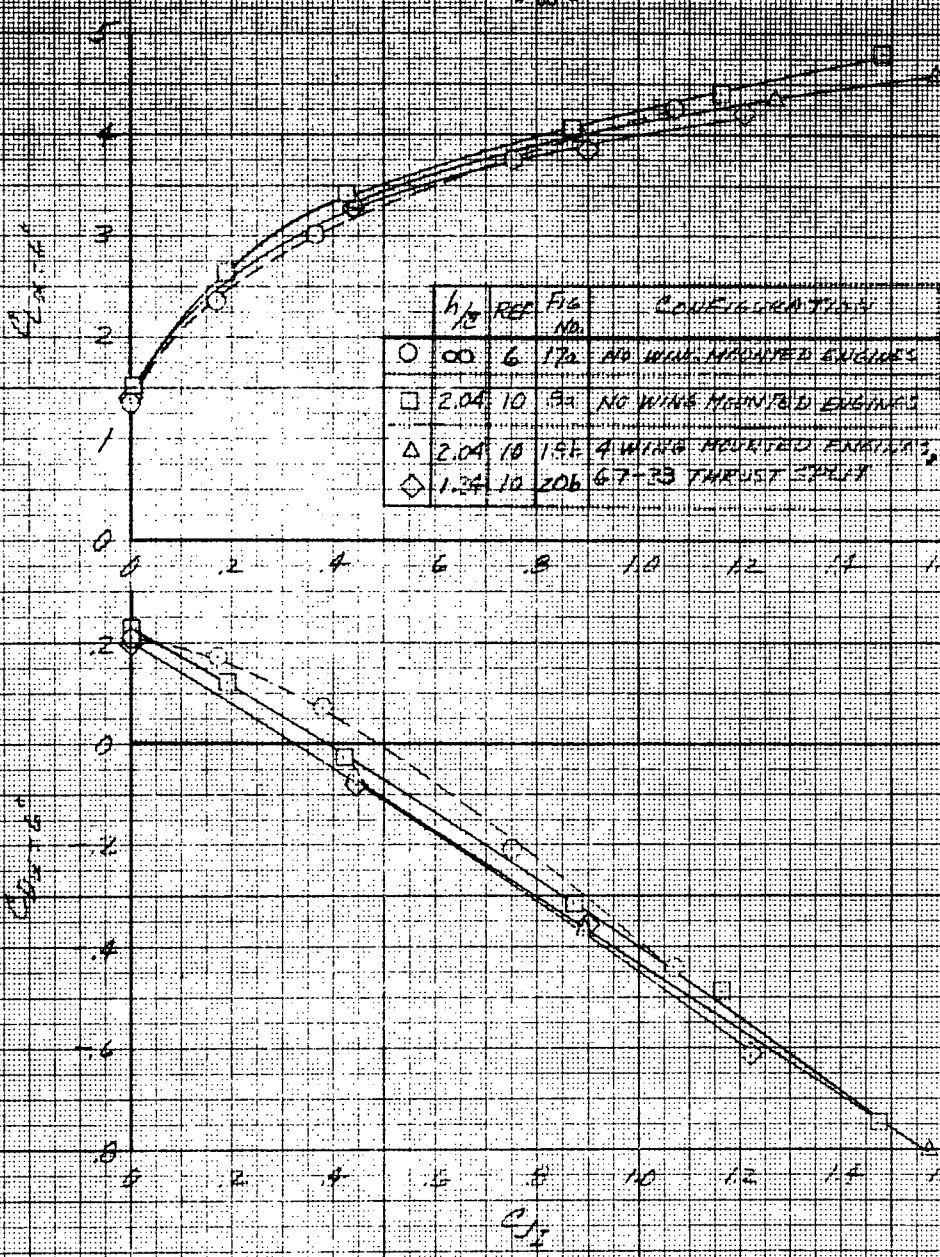

(a) $\delta_f = 40°$, TAIL OFF

FIGURE C2.- EFFECT OF GROUND PROXIMITY AND ENGINE INSTALLATION.

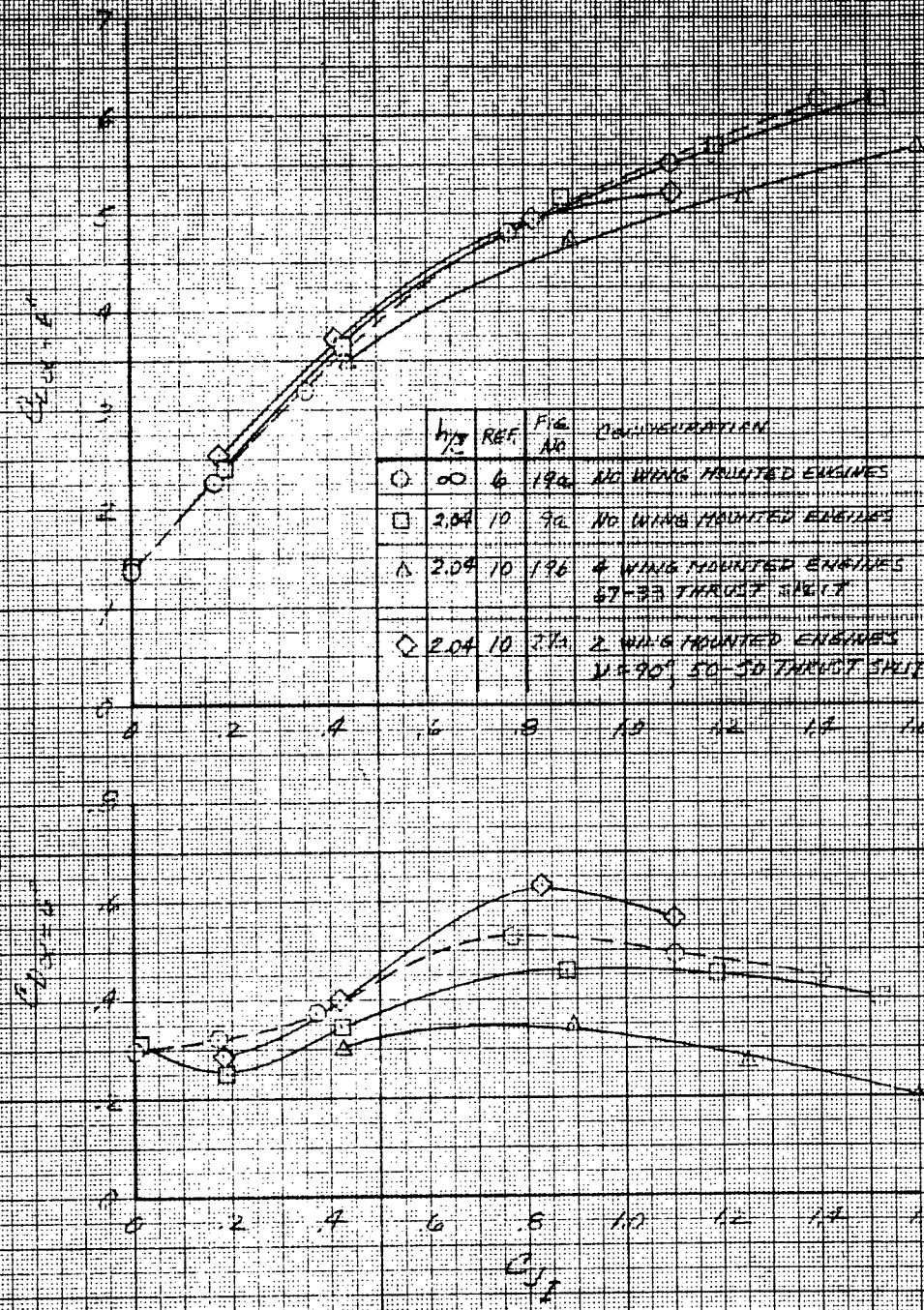

	h/b	REF.	FIG. NO.	CONFIGURATION
○	∞	4	19a	NO WING MOUNTED ENGINES
□	2.04	10	9a	NO WING MOUNTED ENGINES
△	2.04	10	19b	4 WING MOUNTED ENGINES δ_T=33 THRUST SHUT
◇	2.04	10	21a	4 WING MOUNTED ENGINES δ_T=90°, 50-50 THRUST SHUT

TAIL ON

(b) δ_f = 70°, TAIL OFF

FIGURE 22. - CONTINUED.

NASA
AMES RESEARCH CENTER

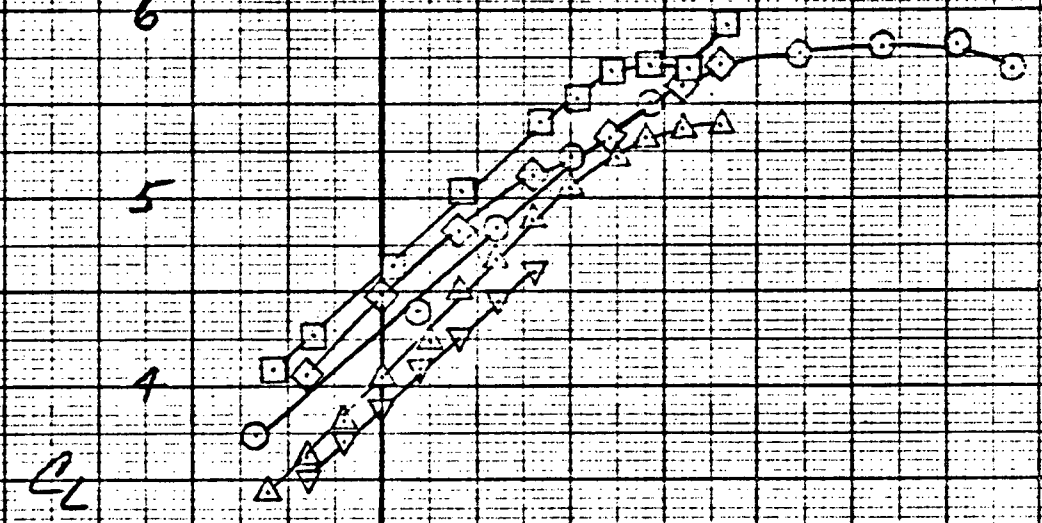

	h/c	C_J	REF	FIG	CONFIGURATION
○	∞	.77	6	19a	NO WING MOUNTED ENG.
□	2.04	.87	10	9a	NO WING MOUNTED ENG.
△	2.04	.89	10	19b	4 WING MOUNTED ENGINES
▽	1.34	.89	10		67-33 THRUST SPLIT *
◇	2.04	.83	10	27a	2 WING MOUNTED ENG. V=90°, 50-50 THRUST SPLIT.

* TAIL ON

(c) $\delta_f = 70°$, TAIL OFF
$C_J = 0.77$ TO 0.89

FIGURE C2. - CONCLUDED.